MODEL-BASED TOOL CONDITION MONITORING
FOR BALL-NOSE END MILLING

HUANG SHENG

NATIONAL UNIVERSITY OF SINGAPORE

2012

MODEL-BASED TOOL CONDITION MONITORING
FOR BALL-NOSE END MILLING

HUANG SHENG

(M.Eng, Huazhong University of Science and Technology)

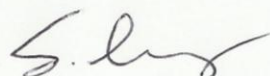A THESIS SUBMITTED

FOR THE DEGREE OF DOCTOR OF PHILOSOPHY

DEPARTMENT OF MECHANICAL ENGINEERING

NATIONAL UNIVERSITY OF SINGAPORE

2012

DECLARATION

I hereby declare that the thesis is my original work and it has been written by me in its entirety. I have duly acknowledged all the sources of information which have been used in the thesis.

This thesis has also not been submitted for any degree in any university previously.

Huang Sheng
31 July 2012

Acknowledgements

I would like to express my sincere gratitude to my research supervisors, Professor Wong Yoke San, Associate Professor Hong Geok Soon, and Professor Zhou Zude, for their constant support, valuable guidance, and great encouragement. I would also like to thank National University of Singapore for offering me excellent research facilities.

I am very grateful to Dr. K. V. R. Subrahmanyam and Dr. He Jing Ming for their support and friendship. I learned a lot from the discussions with them. I would also like to thank my friends, Yu Deping, Wu Yue, and Feng Xiaobing. Their friendship has helped me in many ways.

Special thanks are given to Mdm Teo Lay Tin, Sharen, Miss Yap Swee Ann, Mdm Thong Siew Fah, Mr Tan Choon Huat, Mr Lim Soon Cheong, Mr Wong Chian Long, Mrs Ooi-Toh Chew Hoey, and all other technicians at Advanced Manufacturing Lab and Control and Mechatronics Lab of NUS for their support and assistance.

I am deeply indebted to Professor Jerry Fuh Ying Hsi, Professor Seah Kar Heng, Professor Rahman Mustafizur, Associate Professor Lee Kim Seng, Professor Duan Zhengcheng, Associate Professor Fu Wangyue, Professor Tang Yangping, Dr. Lu Li, Dr. Anton J. R. Aendenroomer, Dr. Goh Kiah Mok, Dr. Li Xiang, and Dr. Lim Beng Siong for their encouragement and understanding.

Finally, I would like to dedicate this thesis to my family for their love and support.

Table of Contents

Summary

In sculptured surface machining, the cutting engagement is not fixed. Most reported or conventional tool condition monitoring methods are based on thresholds or features derived from sensor signals captured from end milling with constant cutting engagement, which are therefore not suitable to be used directly for monitoring sculptured surface machining. On the other hand, several machining models and simulation methods have been developed in sculptured surface machining. These methods are generally applied prior to the cutting process to optimize the milling strategies and cutting parameters. There is a potential to apply the conventional tool condition monitoring methods in sculptured surface machining by accounting for the varying cutting engagement through the use of such developed machining models.

The primary aim of this study is to investigate model-based tool condition monitoring methods for ball-nose end milling targeting for sculptured surface machining applications. The approach is based on a proposed tool wear modelling framework comprising of three parts: cutting force simulation, discrete wavelet analysis of cutting force sensor signal, and feature-based tool wear estimation model.

A discrete mechanistic model is used to simulate the cutting force along the tool path to provide reference features. This model is developed by slicing the cutter into a series of axial discs. Each flute is divided into a few elemental cutting edges and the cutting force is aggregated from that for each elemental cutting edge.

To deduce the tool wear from the cutting force, suitable features are extracted from the measured cutting force and the simulated cutting force. As the engagement condition of the sculptured surface changes, a time-frequency monitoring index based on wavelet transform has been developed and found to be more effective than that based on fast Fourier transform (FFT-based monitoring index). Wavelet transformation requires a smaller time window than FFT, while also provides frequency characteristics of the periodic cutting force signal. The adaptive window width in wavelet transform is an advantage for analyzing and monitoring the rapid transient of the cutting force signal as cutting engagement changes. Daubechies

wavelets are employed and derived from the cutting force during ball-nose milling. The residuals of the wavelets between the simulated force and the measured force signals are used for feature extraction.

Machine learning methods are investigated. By training through examples, a machine learning method can be used to map suitable features (input) derived from the cutting force to the tool wear level (output). Among the machine learning methods, support vector regression (SVR) is a new generation of machine learning algorithm which was developed by Vapnik et al. It is a well-established universal approximator of any multivariate function. Consequently, as a supervised method, SVR has been selected to establish the non-linear relation between the cutting force and tool wear, taking advantage of prior knowledge of the tool wear.

As the tool wear process is complex, there exist complementary, redundant and possibly detrimental interactions between some features in mapping their relation to the tool wear. Hence a proper feature selection process to identify an effective subset can improve efficiency and performance. Rough set theory (RST) is a data mining tool to explore the hidden patterns in the data set. It is based on equivalence relations in the classification of objects. One main advantage of RST data analysis is that it only uses information inside the training data set; that is, it does not rely on prior knowledge, such as prior probabilities. In this investigation, the granularity structure of the cutting force features is studied using RST to find the optimal subset of features from the original set according to a given criterion.

A tool wear estimation framework, has been developed that integrates the cutting force simulation, cutting force signal processing, wavelet feature extraction from cutting force signals, feature selection using RST, and tool wear estimation using SVR. Preliminary experiments to mill inclined surfaces at different inclination angles, different depths of cut and feedrates have been conducted to validate the proposed methods using the developed framework. The experimental results show that the tool wear estimation framework can effectively estimate maximum flank wear over various cutting conditions and inclined surfaces simulating different engagements of the cutting tool.

The milling of a hemispherical surface enables study for tool wear and associated cutting force signals in milling with varying tool engagement. To build an effective model to monitor the tool wear profile in the hemispherical surface milling, a multi-classification and regression method using support vector machine is

investigated. The residual cutting force wavelet features from the measured and simulated cutting forces are used to monitor the change of tool wear profile. Since the effective chip load at different section in the same contact area is varying for each specific tool pass, the geometric modelling method has to be employed to build training data sets to train the SVR tool wear model. The experimental results showed that model-based SVR tool wear estimation method can reflect the non-linear relationship between cutting force and tool wear so that the change of tool wear profile during milling can be monitored.

Keywords: sculptured surface machining, ball-nose end milling, tool condition monitoring, tool wear estimation, mechanistic cutting force model, feature extraction, feature selection, wavelet transform.

List of Tables

List of Figures

Nomenclature

Tool geometry:

D : Diameter of the cutter

R_0 : Tool radius

n_t : Number of teeth on the cutter

β_0 : Helix angle at flute and shank meeting point

κ : Location angle of specific disc

$R(i)$: Local radius at *i-th* disc

ψ : Lag angle of specific disc

β : Local helix angle of specific disc

Tool geometry in terms of chip:

dS : Differential cutting edge length

db : Length of differential cutting edge perpendicular to cutting speed, or chip width in each cutting edge discrete element

t : Instantaneous undeformed chip thickness

Model coefficients:

K_{te}, K_{re}, K_{ae} : Edge force coefficients

K_{tc}, K_{rc}, K_{ac} : Shearing coefficients

K_t, K_r: Cutting mechanics parameter

m_t, m_r: Size effect parameter for most metallic materials

C_w : Edge force coefficient due to flank wear.

Cutting conditions:

f_t : Feed per tooth, feed rate (mm/rev-tooth)

F : Feed rate (mm/min)

N : Spindle speed (revolutions per minute, rpm)

V : Cutting speed ($V = \pi DN$)

a_a: Axial depth of cut

a_r: Radial depth of cut.

VB : Width of flank wear.

γ : Workpiece surface tilt angle from horizontal (deg)

θ : Tool rotation angle, measured from +y-axis clock wise

θ_{st} : Tool entry angle

θ_{ex} : Tool exit angle

θ_p : Tool pitch angle (or tooth spacing angle) ($\theta_p = \dfrac{2\pi}{n_t}$)

ϕ : Instantaneous immersion angle, $\phi = \theta - \psi(z)$ (for each disc)

ϕ_{st} : Tool entry angle (for each disc)

ϕ_{ex} : Tool exit angle (for each disc)

θ_s : Swept angle, the difference between the exit angle of last engaged disc and the entry angle of the first engaged disc, $\theta_s = \theta_{ex} - \theta_{st}$, where the entry angle of the first engaged disc is $\theta_{st} = \phi_{st} + \psi(z_{min})$, the exit angle of last engaged disc is $\theta_{ex} = \phi_{ex} + \psi(z_{max})$.

Rough set theory (RST)

U: a non-empty finite set of objects
A: a non-empty finite set of attributes
d: decision attribute

Chapter 1

Introduction

1.1 Problem statement

Tool condition monitoring (TCM) aims to identify suitable cutting tool conditions using intelligent sensor systems without interrupting the manufacturing process operation. A tool condition includes catastrophic tool failure, collision, progressive tool wear or tool chipping/fracture (Byrne et al., 1995). In TCM, suitable sensing methodology is to be used or developed to monitor these tool conditions. TCM as a monitoring system has the following monitoring scheme:

- Sensor signal capture

- Signal processing

- Feature extraction

- Decision making

The application of this study is to use cutting force sensor to monitor tool wear in ball-nose end milling. The study of tool wear monitoring belongs to the research area of TCM (Dornfeld, 2003).

In ball-nose end milling, the unavoidable tool wear development is one of the major factors that affects the workpiece quality and accuracy. This research is part of an effort to increase the effectiveness in ball-nose end milling by applying a model-based on-line tool wear monitoring method. According to ISO 8688-2 (1989), flank wear is

caused by the progressive loss of tool material at the tool flank during cutting processes. Although tool wear involves a combination of different wear mechanisms, the profile of the flank wear land, including the maximum width and the area of flank wear land in current engagement, is used to quantify and set the criterion for the determination of the tool life in this research.

Generally, tool wear consists of an initial break-in stage, a regular stage and a fast wear stage just before tool breakage (Huang et al., 2007b). During the fast wear stage, the tool wear rate increases rapidly, and finally the tool loses a major portion of the tool edge, causing the failure in the cutting ability of the tool. In order to reduce production cost and improve product quality, the requirement from industry is to monitor the tool wear and warn the operators of the fast wear stage right before tool failure (Jerard et al., 2008). Therefore, compared with off-line tool wear measurement, on-line tool wear estimation has become a very important function in the ball-nose end milling process.

Various sensor-based on-line tool wear estimation methods have been found in recent research literature (Dimla, 2000). The most commonly used approaches include monitoring cutting force, spindle power consumption, acoustic emission, and vibration. Cutting force is an important parameter in measuring the tool condition. The variation in the cutting force can be correlated to tool wear. Due to the intermittent nature of milling process, the cutting force measurement has been shown to be one of the most practical approaches to monitor tool conditions in milling. This method comprises a number of stages, including signal processing, feature extraction and tool wear estimation.

The main challenge in the monitoring of the ball-end milling process is the varying cutting force due to the continuous change in tool-workpiece engagement. As the tool

path for machining is facilitated by the use of the CAD/CAM system, the cutting process along the tool path can be simulated before the actual cutting is performed on the milling machine. After the cutting parameters are extracted through the simulation, the dynamic cutting force can be analyzed from a mechanistic milling force model by the use of geometrical modeling techniques. A mechanistic model has been established in this research to predict the cutting force at the simulation stage when the tool moves along a tool path on the sculptured surface.

Signal processing and feature extraction aim to analyze and process cutting forces to find reliable signal patterns indicating tool wear states (Prickett and Johns, 1999). As tool-workpiece contacts in the milling process have a periodic nature, signal processing and feature extraction can be conducted using either frequency domain method or wavelet transform method. However, the frequency domain method needs sufficient time window on the signal to fulfill the frequency resolution in the power spectrum, and may not be suitable for ball-nose end milling applications. The wavelet transform method requires smaller time window than the frequency domain method, but it can still analyze the frequency pattern of the periodic cutting force signal. The adaptive window width in wavelet transform is an advantage for analyzing and monitoring the rapid transient of small amplitude of cutting force signal when cutting engagement changes along the sculptured surface tool path.

Tool wear estimation is to interpret the information after the cutting forces are processed (Prickett and Grosvenor, 2007). In this research, machine learning methods are proposed for tool wear estimation to map the features (input) to tool wear level (output) by training via examples. The output shows non-linear relations between the input features and tool wear to estimate tool wear in milling applications.

1.2 Motivation

Tool condition monitoring (TCM) is necessary as the surface quality and workpiece accuracy are affected by unavoidable tool wear development besides collisions or tool breakage. From literature, TCM for ball-nose end milling is one of the least researched areas and solutions for ball end finishing operations on sculptured surface are still not available in the market (Dornfeld, 2003). Rehorn et al. (Rehorn et al., 2005) reviewed tool condition monitoring (TCM) researches performed in turning, face milling, drilling, and end milling. After analyzing TCM researches organized by machining operation, they also found that monitoring of end milling operations is the least studied in the four types of machining.

According to Rehorn et al. (2005), tool condition monitoring in ball nose end milling is more complex than that in turning, face milling, and drilling. This conclusion is also supported in another paper (Dornfeld, 2003). Most of the ball-nose end milling applications are machining of complex sculptured surface, especially at finishing stage, which is a very demanding process in mould and die, aerospace, and medical applications. Compared with most recent tool condition monitoring (TCM) methods applied to machining, such as turning, face milling, and drilling, the complexity in the design of TCM for ball nose end milling is:

1) The ball-nose end milling is frequently applied for machining the sculptured surface of workpiece with very complex geometry. Compared with turning, drilling, and face milling, the complexity of TCM method is that the cutting engagement always changes due to the geometrically complex surfaces typically encountered. The standard fixed threshold method is not suitable for ball nose end milling.

2) Most of the applications of ball-nose end milling are very flexible production, such as mould and die production and applications in aerospace industry. In this production environment, the workpieces are manufactured in small batch sizes or one-off production. Consequently, machining conditions change frequently in these applications. Most of commercially available TCM systems are mainly applied in mass production with limited changes of machining conditions. Therefore, flexibility is one of the reasons why there is a lack of tool condition monitoring solutions for ball-nose end milling.

3) As ball-nose end milling is normally one-off or small batch machining, trial machining of some workpieces is time-consuming and very expensive. Therefore, there is a lack of the data of test cuts for different cutting condition.

4) Another complexity is reflected in the small process forces compared with other machining.

Most of present monitoring systems only determine the presence of the fault, that means the decision is either tool worn or tool not worn (Teti et al., 2010). In common industrial practice, the master machinists are able to predict the tool breakage by listening to the cutting or inspecting the chips produced during cutting. In most cases, tool wear does not mean the end of useful tool life. If the tool wear is tolerable, the machinist may decide to continue using the tool in subsequent tool path. Therefore, tool wear monitoring methods need to be developed to overcome the limitation of current monitoring systems. In this way, instead of the master machinist monitoring the tool wear constantly, the threshold-based tool wear monitoring system can monitor the tool condition in real-time. The machinist will be alerted when the machining process needs to be supervised closely when tool wear is over certain limit.

As discussed in section 1.1, presently, sensor based on-line tool wear monitoring solutions in ball-nose end milling are still lacking. There is a need to explore a method to estimate tool wear using cutting force. On the other hand, in ball-nose end milling sculptured surface operation, the engagement between tool and workpiece varies in the milling process. As a result, the cutting forces change with the tool path along the sculptured surface. That means the change of the surface geometry has the same effect as the tool wear on the conventional monitoring indices. Therefore, conventional monitoring indices are not sensitive enough to tool wear in sculpture milling process.

As cutting forces are indirect indication of tool wear, to reliably relate force signals with tool wear is a challenge in this research area. In the monitoring of sculptured surface machining process, conventional features extraction methods are not suitable for use to monitor the tool wear, as the cutting engagement condition changes continuously.

Few researches have been reported using wavelet methods in tool wear estimation. When cutting engagement changes along the sculptured surface tool path, the adaptive window width in wavelet transform is an advantage for analyzing and monitoring the rapid transient of small amplitude of cutting force signal.

1.3 Objectives and scope of work

The aim of the study is to develop model-based tool condition monitoring methods for ball-nose end milling. The methods will combine wavelet-based feature extraction and model-based engagement analysis techniques to monitor tool wear in ball-nose end milling. The specific objectives are:

(1) To simulate cutting forces in ball-nose end milling using a mechanistic model;

(2) To extract features from the force signals which are sensitive to flank wear based on the cutting force model;

(3) To apply suitable machine learning methods to determine the tool wear values with the combination of the simulated features and the measured features.

The measured and simulated instantaneous cutting forces during the milling process are processed on-line to obtain measured and simulated feature vectors. The residual feature vectors can be used for tool condition identification by machine learning methods. Cutting force modelling and wavelet signal processing techniques can be explored to extract sensitive monitoring features. Presently, several cutting force models and simulation methods have been developed in sculptured surface machining. These methods are only applied prior to the cutting process to optimize the milling strategies and cutting parameters. Combined with the geometric modelling of the surface, the cutting engagement along the cutting tool path can be extracted, and the dynamic cutting force can be simulated using milling force model.

The development of a model-based tool condition monitoring method for ball-nose end milling is proposed in this research. This method plays an important role in the reduction of production cost and the improvement of product quality, particularly in mould and die and aerospace industry.

To achieve the objectives, the scope of work includes:

(1) Designing experiments for development of tool condition monitoring methods. In the experiments, cutting forces are measured through the workpiece using a force dynamometer and tool wear is quantified by studying flank wear.

(2) Monitoring and determining tool wear with a cutting force model. The cutting force along the machining path is simulated by a discrete mechanistic model.

(3) Determining effective quantitative monitoring indices that reflect the transient nature in ball-nose end milling sculptured surface. Features for tool wear estimation are extracted by using wavelet transform.

(4) Support vector machines for regression (SVR) and other suitable neural networks will be studied and used for tool wear estimation.

1.4 Organization of the thesis

This thesis is organized into six chapters as follows:

- Chapter 2 is a review of literature on tool condition monitoring, covering sensors for tool condition monitoring, cutting force modeling for ball-nose end milling, signal processing, feature extraction and selection and tool wear monitoring methods.

- Chapter 3 presents a tool wear estimation framework. The approach is based on a proposed tool wear modelling framework comprising of three parts: cutting force simulation, discrete wavelet analysis of cutting force sensor signal, and feature-based tool wear estimation model.

- Chapter 4 describes a feature selection method to improve the tool wear estimation accuracy. Rough set theory is used to reduce attributes of the decision table which is the input of the tool wear estimation model.

- Chapter 5 presents the development of the tool wear estimation framework in ball nose end milling of the hemispherical surface which presents variable tool-workpiece engagement.

- Chapter 6 concludes the thesis with a summary of the contributions and suggestions for future work.

Chapter 2

Literature Review

2.1 Overview

In this chapter, tool condition monitoring researches are reviewed covering sensors for tool condition monitoring, cutting force modeling for ball-nose end milling, signal processing, feature extraction and selection, and decision making for tool condition monitoring methods. References related to tool wear monitoring in milling are emphasized in the literature review. The literature review is arranged in the following sections:

2.2 Tool condition monitoring system

Firstly, commercial tool condition monitoring systems are introduced in this section. Secondly, tool condition monitoring methods in ball-nose end milling are presented.

2.3 Sensors in tool condition monitoring

As the interactions between the machines, workpieces, human operators and environment in machining are very complex, employing appropriate sensors is very important for sensor-based tool condition monitoring systems to ensure effective production and protect operators and the environment. Various sensing methods for tool condition monitoring in milling are reviewed. In those applications, sensors are employed to monitor tool condition by measuring cutting force, spindle power consumption, and vibration.

2.4 Cutting force model for ball-nose end milling

The aim of this study is to investigate model-based tool condition monitoring methods for ball-nose end milling. Therefore, empirical cutting force model and mechanistic cutting force model methods for ball-nose end milling are introduced in this section.

2.5 Signal processing and feature extraction

In TCM applications, tool condition is monitored by capturing sensor signals on-line. As sensor signals are convoluted with noise from the machine, appropriate feature extraction methods need to be explored to maximize the information utilization of sensor signals. These features are used as inputs of the decision making module. Various feature extraction methods in the literature are introduced in this section. Features can be extracted from sensor signals in time domain, frequency domain and time-frequency domain. In time domain, statistical features such as mean, variance, RMS are used as real-time monitoring indices. If the sensor signal has periodic nature, features can be extracted in frequency domain in a specific frequency band. For those sensor signals with rapid transient nature, time-frequency domain features such as wavelet coefficients are more sensitive due to adaptive window width. The similarity between the wavelet coefficients of measured signal and reference signal is a kind of sensitive feature. The similarity can be calculated in many ways, such as Euclidean distance, Mahalanobis distance (MD), and correlation distance.

2.6 Feature selection

In the feature extraction, the features are extracted from cutting force signals for tool wear estimation. The sensitivity of the features to the tool wear needs to be evaluated in order to select high sensitivity features and avoid redundant features.

2.7 Decision making

The decision making function is to build models between the extracted features and tool conditions. Some decision making methods for TCM, such as threshold method, regression method, and hidden Markov model are introduced.

2.8 Neural network methods for tool condition monitoring

Neural network approaches have been used in tool condition monitoring because of their learning capability. Five types of neural networks used in tool condition monitoring are introduced in this section: multilayer perceptron (MLP) network, radial basis function (RBF) network, support vector machine (SVM), adaptive resonance theory (ART2), and self-organizing map (SOM).

2.2 Tool condition monitoring

Current commercial tool condition monitoring systems can monitor tool breakage, tool presence, tool wear and collision in real time (Jemielniak, 1999). Some of the major companies that provide tool condition monitoring systems are Montronix, Inc., Nordmann GmbH, Prometec GmbH and Marposs S.p.A.

Normally, those commercial tool condition monitoring systems use many different sensor types. As reliability is the main concern in the industry, only the most reliable sensor signals, such as power, vibration and force signals are used.

The most common monitoring strategies are based on limits and enveloping functions (O'Donnell et al., 2001). These strategies are suitable for monitoring mass production processes in real time. Before beginning a new batch of the machining operation, a typical machining operation with new cutting tool and new part are conducted while the sensor signals are recorded and stored as reference signals. Based on the reference signals, certain limits and reference pattern are recognized and set up. When the machining operation is conducted, the real-time sensor signals are compared with the reference signals. The tool condition monitoring system will take appropriate action in real time based on the comparison result.

For the implementation of tool condition monitoring, the TCM manufacturers provide in-process tool monitoring solutions that detect changes in the monitored signals at specialized position on the machine. The changes of these signals are sensitive to determine process changes that occur in the manufacturing process. For example, Marposs S.p.A. provides a monitoring system to monitor tool breakage by continual monitoring of the force and spindle power. However, the performance of these systems relies upon the operator and engineer's experience on how to determine the correlation between tool condition and the sensor signals. Sometimes the monitoring system reports alarm due to some change in the process but the cause cannot be identified. Current commercial machining process monitoring applications are not able to handle more complex processes, such as sculptured surface machining.

Two tool condition monitoring methods using cutting force measurements in ball-nose end milling are introduced in this section. One of the methods detects the tool

breakage using a micro-genetic algorithm (GA) during ball-nose end milling operations (Zhu et al., 2003), while the other method recognizes the excessive tool wear through the on-line calculation of the model coefficients (Jerard et al., 2008).

Zhu et al. (2003) undertook an elaborate experimental investigation into the development of a model-based tool fault diagnosis methodology for free-form surface milling process. The tool faults in their work refer to tool run-out, tool chipping and tool breakage in roughing stage. An experimental test bed consists of a horizontal machining centre with a Kistler 9257A 3-component dynamometer. Test cuts were conducted using four-flute carbide ball end mill of diameter 19.05 mm to machine AISI 1018 Steel. A mechanistic cutting force model was developed to simulate the cutting force. Let θ be the rotation angle, the mechanistic force model can be illustrated as follows (Zhu et al., 2001):

$$\begin{bmatrix} Fx(\theta) \\ Fy(\theta) \\ Fz(\theta) \end{bmatrix} = \sum_k \sum_j \begin{bmatrix} dF_x^{jk}[Kn, Kf, K, t_c^{jk}(\theta, \rho, \lambda, CH^k)] \\ dF_y^{jk}[Kn, Kf, K, t_c^{jk}(\theta, \rho, \lambda, CH^k)] \\ dF_z^{jk}[Kn, Kf, K, t_c^{jk}(\theta, \rho, \lambda, CH^k)] \end{bmatrix} \qquad (2.1)$$

where ρ is the amount of parallel axis offset runout in mm. λ is the angle measured at the bottom of the cutter between the direction of the offset and the nearest tooth. CH^k is the chipping magnitude in mm at the kth flute.
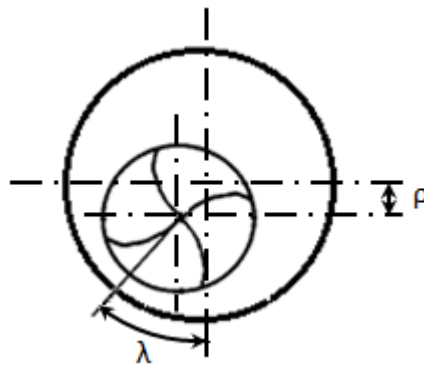
Figure 2.1 Definition of run-out (Zhu et al., 2003)

In the expression of the model, after the coefficients (*Kn, Kf, K*) have been determined in model building experiments, the cutting force at each element (k^{th} flute, j^{th} disc) is a function of undeformed chip thickness (t_c). As the influence of tool run-out and chipping/breakage (ρ, λ, CH^k) is incorporated into the calculation of the undeformed chip thickness (t_c), this model can be used for determining the tool states by neural networks searching algorithm.

A model-based tool fault diagnosis method using a micro-genetic algorithm (GA) is proposed by Zhu et al. (2003).When the measured cutting force and simulated cutting force are processed through wavelet transform, the approximation coefficients A_p representing the signal energy up to four times tooth passing frequency is used as feature vector. The deviation between the simulated feature vector and the measured feature vector is as follows

$$\delta = \sqrt{\sum_{i=1}^{m} [A_p^e(i) - A_p^s(i)]^2} \qquad (2.2)$$

where $(A_p^e(1),\ A_p^e(2),... A_p^e(m))$ is measured feature vector, $(A_p^s(1),\ A_p^s(2),... A_p^s(m))$ is simulated feature vector, *m* is the length of the feature vector, δ is the deviation between the simulated feature vector and the measured feature vector.

Cutting force was processed through wavelet transform. After wavelet decomposition, the approximation coefficients at level *p* were included in the feature vector in (2.2). As the fault information is concentrated in cutting force in the region of low spindle frequency harmonics, the approximation coefficients at level *p* are selected as features to represent the force signal energy up to four times tooth passing frequency. In Eq (2.2), A_p is the feature vector of the approximation coefficients at level *p* after wavelet decomposition. A_p^e is the measured feature vector; A_p^s is the simulated

feature vector. The relationship between the length of the feature vector (m) and the sampling length of the cutting force (n) is: $m = n / 2^p$.

There are two fault variables in the force model, namely, tool run-out (ρ, λ) and chipping/breakage (CH^k). For a certain cutting condition, simulated feature vector with different values of fault variables can be simulated using the cutting force model. Then a search method, such as Genetic Algorithm (GA), can be employed to find the values of fault variables to minimize the deviation in (2.2). In this way, the current fault magnitude can be estimated.

Jerard et al. (2008) explored a tool wear estimation method using the coefficients of a tangential cutting force model. They proposed an online calibration method to monitor tool condition by observing the patterns of the coefficients.

The cutting force model is developed by slicing the cutter into a series of axial discs. Each flute of the tool is divided into a few elemental cutting edges and the cutting force is summed up from each elemental cutting edge. From geometrical point of view, the milling operation on each elemental cutting edge is oblique cutting; so the cutting force on the elemental cutting edge can be considered as a resultant force of three force components. The three force components are differential cutting forces in tangential, radial and axial direction. The instantaneous milling force at a specific disk in tangential direction can be shown to be (Altintas, 2000):

$$dF_t(\phi) = K_{te} \cdot dS + K_{tc} \cdot t(\phi) \cdot db \tag{2.3}$$

where dF_t is the elemental cutting forces, ϕ is rotation angle, dS is the differential length of the curved cutting edge segment, $t(\phi)$ is the undeformed chip thickness normal to the cutting edge, db is the chip width in each cutting edge discrete element,

K_{tc} is the tool/material cutting energy coefficient in the tangential direction, K_{te} is the edge or rubbing coefficient in the tangential direction.

In the cutting force model, the cutting force includes the shearing force component and the ploughing (or rubbing) force component. The shearing force component is the force required to remove the chip. The ploughing force is the force acting on the tool edge and tool flank face (tool-workpiece interface region).

The experimental results with a HSS flat end mill (Xu et al., 2007) showed that as the flank wear land expands, the edge coefficient (K_{te}) increased while cutting energy coefficient (K_{tc}) remaining roughly constant. On the other hand, cutting energy coefficient (K_{tc}) increased as edge chipping and breakage occurs. When the tool wear develops, the ploughing force at the flank of the cutting edge will increase due to the friction between the flank surface and the workpiece. The shearing force will change when the tool wears severely.

The research to incorporate tool wear into the cutting force model is still in progress; this can be understood by the statement (Jerard et al., 2008): "Our current research is focused on developing reliable correlations between the coefficients and the type and extent of tool damage."

2.3 Sensors in tool condition monitoring

A large variety of sensors and various sensing methods for in-process monitoring tool wear and breakage are found in recent research literature (Dimla, 2000). Indirect measurement is the most commonly used approach, which includes monitoring

cutting force, spindle power consumption, acoustic emission, and vibration (Chen and Jen, 2000).

As the interactions between the machines, workpieces, human operators and environment in machining are very complex, employing appropriate sensors is very important for sensor based tool condition monitoring systems to ensure effective production and protect operators and the environment. In terms of sensor requirement for tool condition monitoring, sensor measurement must be as close as possible to the point of metal removal; on the other hand, sensor must not restrict the working space of the milling machine.

The spindle power signal is an indirect way to measure the cutting force. It is considered to be robust. In some applications, the power sensor is not suitable due to the large effects of the inertia and friction in the spindle. Amer et al. (2006) used existing spindle speed and spindle load signals from the machine to monitor tool breakage in the end milling process.

Vibration monitoring techniques applied to the detection of tool breakage have been reported by several investigators. Some researchers suggested power spectrum of vibration data to monitor the tool breakage in end milling process (Huang et al., 2008). Chen and Chen (1999) developed an on-line tool breakage monitoring system using an accelerometer in an end milling operation. Tests were conducted on an aluminum work piece utilizing high-speed steel cutting tool at different spindle speed, feed rates and depth of cut. They found that when tool breakage occurs, the power magnitude at 2nd harmonics of spindle frequency harmonics ($2\omega s$) becomes significant. Based this observation, they proposed the ratio of the two peak magnitude ($P(2\omega s)/P(\omega s)$) as threshold to detect the tool breakage at various conditions. Zhang and Chen (2008) used vibration signal analysis in time domain and frequency domain

to detect tool wear and breakage in end milling process. A microcontroller based data acquisition system was developed for tool condition monitoring. Inspection of the experimental results indicated the vibration amplitudes in time domain and the frequency peaks at harmonic frequency bands to be key indicators of tool condition.

Because the vibrations in machining processes are produced by various mechanisms, one of the main difficulties of detecting tool breakage with vibration is to identify the monitoring index that is influenced by tool breakage. From the literatures the vibration pattern and frequency range sensitive to tool states are entirely different for each individual case, although all the cases are end milling process. Presently, vibration monitoring is only successfully used in specific end milling application with fixed cutting conditions.

Cutting force is an important parameter to measure the tool condition. The variation in the cutting force can be correlated to tool wear. Several researches have shown that the cutting force measurement is one of the most practical approaches to the tool condition monitoring in milling. The cutting force may be measured directly from force sensor (Du, 1999), or may be measured indirectly by measuring spindle power, torque or current. Ritou et al. (2006) presented a versatile monitoring method that use the link between radial eccentricity and cutting forces as indicator to monitor milling tool condition. From literatures, cutting force signals measured using dynamometers is widely accepted (Prickett and Grosvenor, 2007). A dynamometer will be used in this research to monitor the tool condition by using cutting force signals.

2.4 Cutting force model for ball-nose end milling

2.4.1 Empirical modeling of ball nose end milling

Before ball-nose end milling force modelling, a geometric model must be established. The geometric model determines the contact area between the tool, chip and workpiece for each machining path from the tool data and CAD/CAM data (Chang et al., 2006). The resultant milling force is distributed over the contact area (Choi and Jerard, 1998). The cutting force model uses the contact area to determine the cutting forces on the tool by slicing the tool into small discs.

Empirical model is a kind of the discrete cutting force models, which is developed by slicing the cutter into a series of axial discs. The tool geometric model used in empirical model is: each flute of the tool is divided into a few elemental cutting edges and the cutting force is summed up from each elemental cutting edge.

Feng and Menq (1994) presented the estimation of cutting force as

$$F = Kbt^m \tag{2.4}$$

where F is the principal cutting force responsible for the total energy consumed, K is the cutting mechanics parameter, b is the width of cut, t is the undeformed chip thickness, $1 > m > 0$ for most metallic materials, the size effect is explicitly characterized by parameter m.

In the above expression, m is the parameter characterizing the size effect of the workpiece material(Feng and Menq, 1994). It is assumed to be constant for a particular material. Size effect refers to the increase of the specific cutting energy at lower value of undeformed chip thickness. Researchers believe that the tool flank friction and ploughing force are main factors contributing to the size effect (Feng and

Menq, 1994). As the cutting edge of ball nose end mill can be represented by a cylindrical surface between the flank face and the rake face, there exists a ploughing force that acts on the tool edge and the tool flank surface. The existence of the ploughing force can explain the size effect: ploughing force is constant and becomes proportional of the total cutting force as chip thickness decreases. Because the undeformed chip thickness is usually very small in ball nose end milling application, size effect must be taken into account in ball nose end milling cutting force model.

The cutting force on each engaged small disc is combined by the tangential and radial components. The empirical cutting force model is expressed as follows (Feng and Menq, 1994):

$$dF_t = K_t(z) \cdot dz \cdot \left[t(\phi)\right]^{m_t} \tag{2.5}$$

$$dF_r = K_r(z) \cdot dz \cdot \left[t(\phi)\right]^{m_r} \tag{2.6}$$

where dF_t and dF_r are tangential and radial cutting forces on each engaged disk, dz is the width of the cut of the disk along the z direction, ϕ is instantaneous immersion angle, $t(\phi)$ is the undeformed chip thickness, m_t, m_r are constants represented the size effect.

K_t and K_r characterize the cutting mechanics of the engaged disc, and can be approximated by third order polynomial expressions (Feng and Menq, 1994):

$$K_t(z) = a_0 + a_1\left(\frac{z}{R}\right) + a_2\left(\frac{z}{R}\right)^2 + a_3\left(\frac{z}{R}\right)^3 \tag{2.7}$$

$$K_r(z) = c_0 + c_1\left(\frac{z}{R}\right) + c_2\left(\frac{z}{R}\right)^2 + c_3\left(\frac{z}{R}\right)^3 \tag{2.8}$$

where z is the axial distance between tool tip and the engaged disc,

R is the cutter radius,

a_0, a_1, a_2, a_3 are the coefficients of the polynomial,

c_0, c_1, c_2, c_3 are the coefficients of the polynomial.

2.4.2 Mechanistic cutting force model

In order to obtain the reference cutting force for the monitoring of sculptured surface machining process, as the engagement condition changes continuously, a conventional method is to divide the surface into a number of regions and to record cutting force when cutter is in normal condition (Zhu et al., 2003). Based on the reference signals from the milling experiments, different features are extracted for monitoring different cutting process segments in the whole milling process. As this method needs trial machining of some workpieces as pre-recorded reference, it is time-consuming and not suitable for one-off and small batch milling applications typical in sculptured machining operations. To avoid the huge amounts of empirical data collection, cutting force models can be used for tool condition monitoring in sculptured surface machining.

A few mechanistic models have been developed by researchers in previous researches. Lee and Altintas (1996) extended the unified mechanics model to the helical ball-end mill. The flute is divided into small oblique cutting edges and the geometry of each elemental oblique cut is related to the conventional practical machining variables. These models yield accurate cutting forces in specific cutting conditions. However, most consider only the horizontal surface machining. As sculptured surface machining is the main manufacturing application for ball-end

mills, Lamikiz et al. (2004) extended semi-mechanistic model to the case of curved surfaces which are closer to applications used in industry for the production of parts with complicated free-form surfaces.

To calibrate parameters in the cutting force model, there are two main types of force model building approaches in the literatures. One approach is based on oblique cutting analysis to make use of practical orthogonal cutting database. Lee and Altintas (1996) developed a unified mechanics model for helical ball-end mill geometry. The coefficients in the model are obtained from the orthogonal cutting database by using the classical oblique transformation method. Another approach is to determine the coefficient by direct calibration test. Lamikiz et al. (2004) carried out horizontal slot milling characterization test. The average forces were measured and the coefficients were obtained by least square adjustment.

As expensive and time-consuming model calibration is required for most of the model building process, Jerard et al. (2005) presented a calibration method of a tangential force model by using motor spindle power, as motor spindle power can be easily measured without affecting the machining process. Zuperl and Cus et al. (2004) used supervised neural networks to predict cutting forces for ball-end milling operation. A neural network algorithm is developed for use as a direct modelling method, based on a set of input cutting conditions, namely, radial/axial depth of cut, feedrate, and spindle speed. Other parameters such as tool diameter, rake angle, etc. are kept constant. Huang et al. (2007b) proposed a fault detection method based on a cutting force observer model in CNC milling centre. A dominant model plus uncertain terms was derived from the model set and used as an observer.

2.4.3 Cutting force simulation

The geometric simulation is used to determine the intersection between the tool and workpiece when machining the sculptured surface. This instantaneous tool immersion information is necessary for calculating the instantaneous cutting force. For example, Saturley and Spence (2000) presented a method using ACIS solid modeling kernel to simulate the volume swept by the tool.

1) Estimation of cutter contact area

When a sculptured surface, such as the surface of a die, needs to be machined, a collection of geometric models will be created in CAD to describe the surface. Then a series of tool paths represented by CNC codes will be generated by CAM for ball-nose end mill to machine the surface. Therefore, surface representation can be derived from the surface geometric models to simulate the milling engagement (Kim et al., 2000).

One of the suitable surface representations is Z-map. A Z-map is a discrete non-parametric surface representation. It is a 2D array storing the Z-values of the surface at grid points on the XY-plane. The Z-map data are obtained by Z-map sampling on the sculptured surface geometric model.

The Z-map representation is defined as follows (Choi, 1991):

$$\{x(i), y(j), z(i, j)\} \; for \; i \in [0, I], \; j \in [0, J] \tag{2.9}$$

where *i, j* are grid indices and *I, J* are positive grid limits.

Let the size of a square grid is *g*, XY coordinates are expressed as

$$x(i) = x(0) + g \cdot i \; , \quad y(j) = y(0) + g \cdot j \tag{2.10}$$

The definition shows that the die and mold surfaces can be modeled as Z-maps. The data structure can be used to develop efficient algorithms to calculate the tool-workpiece boundary to simulate the ball-nose end mill plunging into the part surface.

2) Cutting force simulation

A cutter plane is defined as a plane perpendicular to the cutter axis in the cylindrical portion. The cutter contact area can be obtained by comparing the Z-map of the surface and the Z axis value of the cutter. The cutting edge need to be projected onto the cutter plane to determine the engagement of the cutting edge (Kim et al., 2003). Assume that the helical ball-end milling cutter is ground with a constant helix lead and a point P located on the helical flute has Cartesian coordinate (x, y, z). If the helix angle of the flutes at the ball-shank meeting boundary is β_0, the rotation angle ϕ at point P is as follows (Kim et al., 2003):

$$\phi = \theta - (1 - \cos(\kappa)) \tan(\beta_0) \qquad (2.11)$$

Then the point P can be projected onto the cutter plane and the *x, y* coordinates can be calculated as follows (Kim et al., 2003):

$$x = R_0 \cos \kappa \cos(\theta - (1 - \cos(\kappa)) \tan(\beta_0)) \qquad (2.12)$$

$$y = R_0 \cos \kappa \sin(\theta - (1 - \cos(\kappa)) \tan(\beta_0)) \qquad (2.13)$$

If the calculated position is within the cutter-workpiece contact area, the cutting edge on this disk engages in the cutting process. Then instantaneous cutting forces are calculated by numerical integration (Kim and Chu, 2004).

2.5 Signal processing and feature extraction

As the cutting force signals in the ball-nose end milling process are very noisy, they need to be processed to identify the tool wear status. Many research works have been conducted to process sensor signals in time domain, frequency domain and time-frequency domain.

In time domain signal processing approaches, it is assumed that the change of the sensor signals is in a steady manner. Although the time domain method is easy to implement compared with frequency domain and time-frequency domain, it is not sensitive to tool wear as cutting engagement always changes. As tool-workpiece contacts in milling process have periodic nature, frequency domain and time-frequency domain can be used to analyze and process cutting forces, so that some reliable signal patterns indicating the tool states can be found (Prickett and Johns, 1999).

Frequency domain analysis techniques in tool condition monitoring have been adopted for some milling applications with fixed engagement by different researchers (Siddiqui et al., 2007). Sarhan et al. (2001) investigated the effect of wear variation on the magnitude of the cutting force harmonics in end milling. Their results showed that using the frequency domain signal processing could reduce the effect of noise on the correlation between cutting force and tool wear. Suprock et al. (2007) analyzed the combination of force signal and vibration signal to track the health of cutting tools. They suggested that the magnitude of certain harmonics of the cutting force increased significantly with tool wear. As frequency domain method needs certain time window on the signal to fulfill the resolution of the frequencies in the power spectrum, it is only suitable for near constant engagement conditions.

Frequency domain techniques such as spectrum analysis have been adopted to form monitoring indices to monitor tool breakage. Table 2.1 shows the observation by Zhu et al. (2003), which can be used to detect tool run-out and chipping/breakage. The monitoring index is calculated along the tool path based on the cutting force simulation. The reason of the observation is: in milling operation, each tooth of the tool enters and exits the workpiece once every revolution. When the tooth of the cutter contacts the workpiece, the cutting action causes a periodic impact force on the contact area with tooth passing frequency on every rotation. If one of the teeth is broken, the following tooth will have more loads to remove extra materials, and the cutting force pattern will change according to the loads change.

Table 2.1 Observation of the sum of power spectrum components

	Tooth passing frequency	ω_s	$2\omega_s$	$3\omega_s$
Normal	x			
Run-out		x		x
Chipping			x	
Run-out & chipping		x	x	x

"x" means the power components become significant at such frequency.
ω_s is the spindle frequency.

In recent years, time-frequency analysis techniques, such as the Short-Time Fourier Transform (STFT), wavelet transform, and Hilbert-Huang transform (HHT) have been investigated in feature extraction from non-stationary, non-linear (transient) signals. These methods are useful to form monitoring indices to monitor tool condition.

Traditional signal processing approaches are suitable for stationary cutting force signals. However, due to the nature of ball-nose end milling processes, the cutting force signals are usually non-stationary (Zhu et al., 2009b). In cases where the engagement condition of sculptured surface always changes, time-frequency features,

such as wavelet transform (WT), are more effective than frequency domain features. WT requires smaller time window than frequency domain features, but it can still analyze frequency pattern of the periodic cutting force signal. Klocke et al. (2000) evaluated the cutting force signals in time, frequency and wavelet domain for monitoring ball-nose end milling. They found that the wavelet coefficients were the most sensitive features to the occurrence of tool wear. Choi et al. (2004) used the root mean square (RMS) value of the wavelet coefficients of resultant cutting force for tool wear estimation in end milling. Although very few researches were reported using wavelet in tool wear estimation, these researches were significant as they tried to make use of the adaptive window width in wavelet transform to analyze and monitor the rapid transient of small amplitude of cutting force signal when cutting engagement changes along the sculptured surface tool path.

Due to the complexity of the ball-nose end milling process, the cutting force signals may not indicate the cutting conditions directly. Features from the cutting force signals need to be extracted to identify the tool conditions.

Ghosh et al. (2007) extracted different features from root mean square (RMS) of cutting forces to estimate tool wear in face milling. But this method is only suitable for very steady machining process such as face milling. Bhattacharyya et al. (2007) found that the correlation between tool wear and average signal energy (ASE) of cutting force was very high. But this correlation is not linear and the result can be easily affected by noise. Zhou et al. (2009) selected time domain and frequency domain cutting force features: average force, total amplitude, standard deviation , and total harmonic power. Li et al. (2009) used four time domain cutting force features as input of the tool wear estimation model: maximum force, average force, total amplitude of force, and standard deviation of force. These features were selected from

sixteen features using a complex feature selection method; however, the experimental data were not sufficient.

2.6 Feature selection

In the feature extraction, the features are extracted from cutting force signals for tool wear estimation. The sensitivity of the features to the tool wear needs to be evaluated in order to select high sensitivity features and avoid redundant features. For example, Dong et al. (2006) extracted some features from cutting force signals of face milling. They used automatic relevance determination (ARD) algorithm to select relevant features to estimate tool wear. Zhou et al. (2009) developed a dominant feature selection method to reduce feature space.

Presently, rough set theory (RST) has been explored by researchers to eliminate redundant features from the original set of features. RST was introduced by Zdzisław Pawlak (Pawlak, 1991) to deal with imprecise or vague concepts. It can be used as a data mining tool to explore the hidden patterns in the data set. It has been used in fault diagnosis to reduce the number of conditional attributes (Huang et al., 2005, Shen et al., 2000). It is based on equivalence relations in the classification of objects. Therefore, rough set theory (RST) was explored as a tool in this work for selection of training data set and reduction of feature space.

Swiniarski and Skowron (2003) showed that rough set method was able to reduce the pattern dimensionality substantially for a classification of face images.

The feature selection method using rough set is to construct a discernibility function from the data set and to find minimal reducts (Wang et al., 2007b).

To use RST for feature selection, the decision table can be used to find reducts and one of the reducts can be used to replace the original table. Normally, a reduct with minimal number of attributes is used as feature selection results (Thangavel and Pethalakshmi, 2009). The research topic is how to develop an effective algorithm to find reducts based on cutting force features.

The advantage of RST is the abilities of dealing with uncertainty inputs (Widodo and Yang, 2007). Therefore, RST is suitable for the constant changing of the engagement when cutting sculptured surface. An integrated feature selection methodology of rough set theory and support vector machine is proposed in this research.

2.7 Decision making

After the cutting force signals are acquired from the sensors, it is necessary to interpret the data for on-line tool wear monitoring in milling processes. A threshold-based cutting tool fault detection method has been developed based on the cutting force model (Huang et al., 2007a). The threshold curve can be obtained off-line based on the process model as the cutting engagement conditions along the tool path are determined at the simulation stage. This is an adaptive threshold value which can be developed through the cutting force model without a trial cut under varying cutting conditions. The measured cutting forces are monitored on-line to detect the faults by comparing them with the threshold curve at machining stage.

The regression method is one of the important methods used to estimate tool wear. Bhattacharyya et al. (2007) used average signal energy features to train multiple linear regression (MLP) model to estimate the tool wear in face milling process. Zhou et al. (2009) proposed a recursive least squares (RLS) method to build a tool wear

regressive model. While the general regression methods are very accurate, they are only suitable for steady cutting operation such as face milling process.

A hidden Markov model (HMM) is a statistical Markov model that consists of a finite set of "hidden" states that are traversed according to certain state transition probabilities. HMM is able to capture the dynamics of a sequence of signatures by state transition probabilities. HMM is used to model the sensor features to monitor the tool condition. Zhu et al. (2009a) proposed an appropriate selection of continuous HMM structure for multi-category tool flank wear state identification in micro-milling based on cutting force. To build a noise-robust solution, the HMM outputs are connected via a medium filter to minimize the possible premature state changing due to noisy signal in the left–right HMMs. In machining, there are three tool wear states: initial tool wear, gradual tool wear, and accelerated tool wear. Tool wear always increases from initial tool wear to accelerated tool wear. Hence the left-right HMM was chosen in their study. Tool state in the left-right HMM can transit to itself and later state, but not to the former state. In the multi-rate modeling, tool state of the classification may enter into the next state because of the noise and cannot change back to correct state. To eliminate this problem, a 15-point moving medium filter is introduced in the HMM recognition. The consecutive 15-state estimations are held to find the medium of these 15 estimates. The final tool wear state is the medium state.

2.8 Neural network methods for tool condition monitoring

An artificial neural network (NN) is a computational model of human brain (Teti et al., 2010). It is a massively parallel distributed processor. It is made up of interconnected neurons for storing knowledge and making the knowledge available

for use. In neural network, the acquired knowledge is stored in interneuron connection strengths which is called synaptic weights (Haykin, 1999). Knowledge is captured from examples through a training process. The synaptic weights of the network are modified in the training process. There are two types of training process: supervised training and unsupervised training. Supervised training means that some neural network can be trained by labeled training samples. The set of training samples contains elements which consist of paired values of the independent (input) variable and the dependent (output) variable. The synaptic weights of the network are modified to minimize the difference between the desired output and the actual output of the network. After training, the neural network should produce reasonable outputs for inputs not encountered during training.

Neural network approaches have been used in tool condition monitoring because of their learning capability. Li et al. (Li et al., 1998) developed a parallel multi-ART2 neural network was developed to detect tool failure and chatter in turning. Kuo and Cohen (Kuo and Cohen, 1999) integrated artificial neural networks (ANN) and fuzzy logic to build a fuzzy neural network (FNN) model to estimate tool wear in turning. Balazinski et al. (Balazinski et al., 2002) applied an artificial neural network-based fuzzy inference system to monitor tool condition in turning. Salgado and Alonso (Salgado and Alonso, 2007) used least squares version of support vector machines (LS-SVM) for on-line tool wear monitoring in turning.

Five types of neural networks used in tool condition monitoring are introduced in this section: multilayer perceptron (MLP) network, radial basis function (RBF) network, support vector machine (SVM), adaptive resonance theory (ART2), and self-organizing map (SOM).

Multilayer perceptron (MLP) network is a multilayer feed-forward network consists of an input layer of source nodes, one or more hidden layers of computation nodes, and an output layer of computation nodes. Smooth nonlinear activation functions are used in the network. MLP network is trained in a supervised manner with back-propagation algorithm. Back-propagation learning consists of a forward pass and a backward pass through the different layers of the network. In the forward pass, an input vector is applied to the network, and an error signal is produced by subtracting the actual output of the network from a desired output. In the backward pass, the error signal is used to adjust the synaptic weights in accordance with an error-correction rule. MLP has ability to solve problems stochastically, which is very useful in tool condition monitoring research to get approximate solutions for complex machining processes.

Chen et al. (Chen and Jen, 2000) developed a tool condition monitoring system using MLP. This system is to monitor tool wear in milling using cutting force and vibration signals. Features were extracted from average value, variation of amplitude, and variation of fluctuating local frequency. The input of the neural network was designed to have 13 input variables including features, operating parameters, and wear grade. In their study, they found that the three-layer architecture had lower training efficiency and test performance than the four- and five-layer architectures. They also used MLP to evaluate five different data fusion methods. The training efficiency and test performance of different data fusion methods were compared by evaluating the convergence speed and the test error. The convergence speed was quantitatively evaluated by comparing the required number of training cycles for approaching an allowable average error. The test error was the error being converged for the same number of training cycles with the inputs from different data fusion method. The

average and standard deviation of the test error were calculated to evaluate the test performance of different data fusion method. Ghosh et al. (2007) developed an MLP model for tool wear estimation in face milling. Their results showed good accuracy in estimating tool wear using the RMS of cutting forces. Their study also revealed that neural network based model has limitation in machining application as the data set is small. In order to overcome the drawback of MLP, Li et al. (2009) proposed a fuzzy neural network modeling method for tool wear estimation in ball nose end milling an inclined surface. However, this method is only applicable for fixed cutting parameters.

A radial basis function (RBF) network is an artificial neural network that uses radial basis functions as activation functions. The design of radial-basis function network can be viewed as a curve-fitting problem in a high-dimensional space. RBF is a feed-forward networks with three layers in the most basic form. The input layer is made up of source nodes. The second layer is the only hidden layer of high dimensionality that implements a set of radial basis functions (e.g. Gaussian functions). The output layer is a linear combination of radial basis functions. The network training is divided into two stages: first the weights from the input to hidden layer are determined, and then the weights from the hidden to output layer. The training is to find a surface in a multidimensional space that provides a best fit to the training data. The tool wear prediction capabilities of the RBF network have been studied using Gaussian functions as the activation function.

Kuo and Cohen (Kuo and Cohen, 1999) tried to correlate tool flank wear in turning to the signals of multiple sensors: acoustic emission, vibration, and cutting force. Features were extracted by the time series analyzer and the frequency analyzer. They employed a radial basis function (RBF) network for recognizing the extracted features

for each sensor. The features and cutting time, speed, and feed were used as the inputs to the RBF network. The basis function in the hidden layer was the Gaussian function which produced a localized response to the input. The output formed a linear combination of the basis (kernel) functions computed by the hidden units. For example, the RBF network architecture consisted of eight input units for the features from the frequency analyzer. The inputs were connected to sixteen hidden units. The hidden units were connected to one tool wear output unit. They evaluated the root mean square error (RMSE) values between the tool flank wear modeled with a candidate feature and the measured tool flank wear value. If the RBF network can learn from one set of features with fast speed and predict tool flank wear in better accuracy than other feature sets, this set of features were selected for tool wear modeling.

Support vector machine (SVM) is another possible way for tool condition monitoring. SVM is based on statistical learning theory (Vapnik, 1998). In a recent publication, Cho et al. (2005) applied support vector machines for regression (SVR) to determine tool breakage. In their research, SVR was used to model the power and maximum cutting force in an end milling application. They found that the SVR approach was better than multiple variable regression (MVR) approach. Bhattacharyya and Sanadhya (2006) used SVR method to model the correlation between the cutting force signal and the tool wear. Although this method was only explored when cutter-workpiece contact area was fixed, it shows a potential that the method could be applied at sculptured surface milling when cutter-workpiece contact area was changed continuously. Dong et al. (2006) implemented two nonlinear regressive models to describe the dependence of flank wear (VB) on cutting force feature vectors in face milling applications. They compared the performance of Bayesian multilayer

perceptrons (BMLP) and Bayesian support vector machines for regression (BSVR), and found that BSVR method was more accurate than BMLP in estimating flank wear.

Sun et al. (Sun et al., 2004b) proposed a tool condition monitoring method using support vector machines (SVM) based on acoustic emission (AE) sensing. This method can perform multiclassification of tool flank wear states in turning. In machining, tool wear process has 3 states: initial tool wear (sharp state), gradual tool wear (usable state), and accelerated tool wear (severe worn state). Binary classification of tool states (normal tool state and worn tool state) may not reflect this wearing process. Hence multiclassification of tool conditions can improve the reliability and validity of tool condition identification. Two different losses due to misclassification were analyzed. Under prediction can result in early tool changing. Over prediction can result in damage of the workpiece by using a worn tool in machining. Hence the losses from different class due to misclassification are different. They designed a revised SVM algorithm with two regularization parameters in objective function to punish the classification error of two classes respectively. This design introduced the potential manufacturing loss into the SVM algorithm. It overcomes the limitation of standard SVM algorithm which assumes that the losses are the same. In their study, one-versus-one method was adopted to perform the multiclassification of tool states. One-versus-one method is suitable for practical use as it has good testing accuracy and fast training time. Three binary revised SVM classifiers are utilized for every pair of three tool wear states. A "Max-Wins" voting strategy is used to implement the one-versus-one method to perform the multiclassification of tool conditions.

The ART2 is an unsupervised neural network with an adaptive resonance theory (ART) architecture. The system consists of two layers, an input representation layer F1 and a category representation layer F2. They are linked by feed-forward and feedback weight connections. After an input pattern is presented to F1 layer, it undergoes a process of activation. The result is sent to F2 layer to produce activation. The best matching pattern is the winner in stored pattern at F2 layer. The best matching pattern is then sent back to the F1 layer through feedback weights. If the winner pattern matches the input pattern, the neural network enters a resonant state to adapt the stored winner pattern. If the winner pattern does not match the input pattern, the neural network will assign an uncommitted node on the F2 layer to this new input pattern.

Niu et al. (Niu et al., 1998) applied adaptive resonance theory (ART2) neural network to identify tool wear status in turning process over a wide range of machining conditions. They analyzed acoustic emission signals using wavelet packet decomposition method to extract spectral and statistical features. This application shows that unsupervised classification and clustering methods are useful when wear measurement is not available to form training pairs.

A parallel multi-ART2 neural network (Li et al., 1998) was developed to recognize tool conditions and machining chatter in turning operations. The parallel multi-ART2 neural network consists of four parallel ART2 sub-networks with the binary outputs. These sub-networks are employed to identify four categories of states: machining chatter, tool failure, simultaneous severe tool wear and chatter, and normal. That means one sub-network is employed to identify one category of state. During the training process, the test samples are grouped according to different categories to train

respective sub-network. After training, the F2 cells within one ART2 sub-network characterize the typical cases of one respective category.

For single ART2 neural network, a single vigilance threshold needs to be set to classify four complex categories. However, for parallel multi-ART2 neural network, four finer vigilance thresholds for the four ART2 sub-networks are employed. In this way, parallel multi-ART2 neural network overcomes the limitation of single ART2 neural network and can be more reliable identification of a variety of complex patterns.

Self-organizing map (SOM) is a special class of artificial neural networks in which the neurons are placed at the nodes of a lattice. The coordinates of the neurons in the lattice are indicative of intrinsic statistical features contained in the input patterns (Haykin, 1999). A topographic map is formed by transforming high-dimensional input patterns into a low-dimensional discrete map where the location of a unit represents the density of the input data. The feature map provides a good approximation to the input space.

Wang et al. (Wang et al., 2007a) proposed SOM for online monitoring of tool wear. In their study, SOM was used to map the patterns of force features to an output unit, and the flank wear was estimated accordingly.

The SOM network was trained in a batch mode after each cutting pass using cutting force features and measured tool wear. Two features were extracted from cutting force. The cutting force features were extracted using the average force and the standard deviation over one rotation. The features are extracted pass by pass. The measured wear values were obtained by interpolating the vision-based measurements.

The vision-based tool wear measurement was obtained by processing the tool images captured in-cycle.

The output of SOM is wear increment value with respect to the measured wear value at the beginning of each pass. The wear value at the beginning of each pass is measured by an automatic vision-based image-processing technique. The predicted absolute wear is the sum of the wear increment value and the initial measured wear value of each pass.

One of the advantages of this application is that only a small portion of input features are needed for supervised learning together with the outputs. Other input data can be used in unsupervised learning. They used labeled and unlabeled input data for asymmetric mapping. Labeled data consists of force features and wear increment value. Unlabeled data consists of force features only.

Another advantage is on-line training. As the worn tool is replaced before the end of the tool wear stable stage, the force signal at this stage is stable and the force features in the previous machining pass can be used to train the SOM network for the flank wear estimation in the succeeding machining pass. In this way, the training can be conducted on-line and cutting conditions are not involved in the training.

In summary, the use of indirect tool condition monitoring methods requires accurate predictive models that link the undetectable tool wear to the detectable sensory signal in the machining process (Teti et al., 2010). Empirically based on-line TCM systems are dependent on large amounts of experimental data and do not take account of the complex nature of the metal cutting operation (Dimla Jr et al., 1997). On the other hand, neural network is an effective method to monitor tool condition for small size productions, especially in milling (Dornfeld, 2003). Neural networks are robust and

capable of non-linear modelling because of their learning capability. Neural network methods have a mathematical background and theory to get approximate solutions for complex machining processes. Some merits of neural network methods in tool condition monitoring applications are data-driven nature, noise suppression capabilities, and fault tolerance and adaptability.

As tool wear is a highly non-linear process, methods based on neural network are explored in this study to find a viable and reliable way to monitor tool wear. Among the NN methods reviewed in this section, support vector machine (SVM) could be a suitable method to be applied in the milling tool wear monitoring to take advantage of prior knowledge of tool wear and construct a hyper-plane as the decision surface (Sun et al., 2004a). As a supervised method, SVM guarantees that the local and global optimal solutions are exactly the same (Widodo and Yang, 2007). SVM can be used for classification and regression analysis. SVM for regression (SVR) is a new generation of machine learning algorithm which was developed by Vapnik et al. (1998). It is a well-established universal approximator of any multivariate function. Compared with multilayer perceptron (MLP) network, SVR has better generalization and higher accuracy for a smaller number of samples. It also overcomes the over-parameterization and non-convergence problems (Bhattacharyya and Sanadhya, 2006). In this study, SVR has been selected to establish the non-linear relation between the cutting force and tool wear.

Chapter 3

Model-based Tool Wear Monitoring

3.1 Introduction

In this chapter, a model-based tool condition monitoring approach is presented for ball-nose end milling. This approach is based on a proposed tool wear modelling framework comprising of three parts: cutting force simulation, discrete wavelet analysis of cutting force sensor signal, and feature-based tool wear estimation model. A discrete mechanistic model is used to simulate the cutting force along the tool path to provide reference features. This model is developed by slicing the cutter into a series of axial discs. Each flute is divided into a few elemental cutting edges and the cutting force is aggregated from that for each elemental cutting edge. To deduce the tool wear from the cutting force, suitable features are extracted from the measured cutting force and the simulated cutting force. As the engagement condition of the sculptured surface changes, a time-frequency monitoring index based on wavelet transform has been developed. Daubechies wavelets are employed and derived from the cutting force during ball-nose milling. The residuals of the wavelets between the simulated force and the measured force signals are used for feature extraction. Machine learning methods are investigated. By training through examples, a machine learning method can be used to map suitable features (input) derived from the cutting force to the tool wear level (output). Among the machine learning methods, support vector regression (SVR) is a new generation of machine learning algorithm which was developed by Vapnik et al. (Widodo and Yang, 2007). It is a well-established

universal approximator of any multivariate function. Consequently, as a supervised method, SVR has been selected to establish the non-linear relation between the cutting force and tool wear, taking advantage of prior knowledge of the tool wear.

3.2 Model-based tool wear monitoring framework
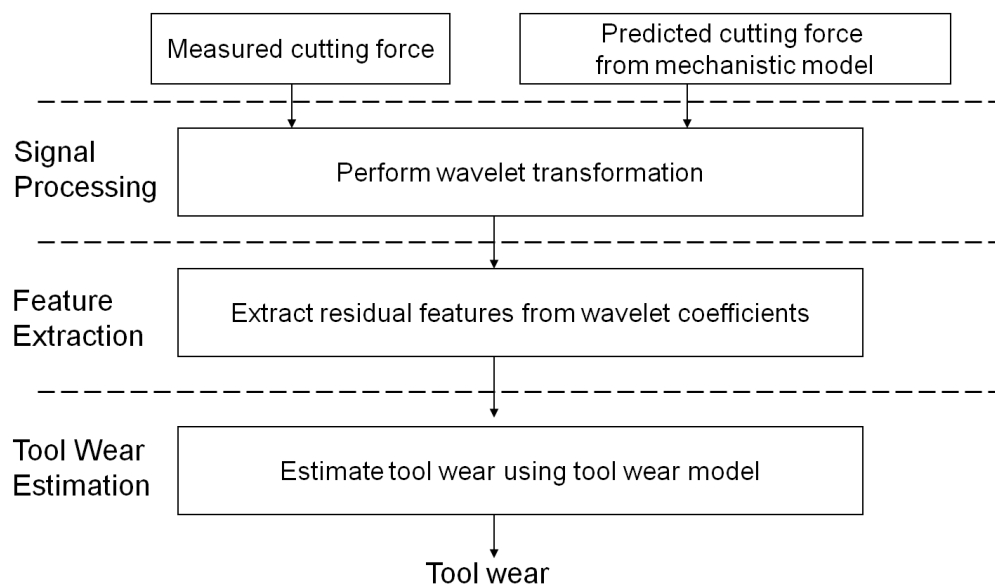
Figure 3.1 Model-based tool condition monitoring

Figure 3.1 shows the proposed structure of model-based tool condition monitoring system. The research effort will focus on following techniques for tool condition monitoring:

(1) A cutting force model (Subrahmanyam et al., 2007) is adopted to simulate the cutting force when the tool moves along a tool path on sculptured surface. This provides the reference cutting force when the tool is in normal condition. The milling process is simulated by the use of geometrical model and cutting parameters along the tool path, such as the feed rate, depth of cut and cutting

speed. By using simulation, huge amount of experimental data collection can be avoided.

(2) The measured and simulated cutting forces are processed by wavelet transform.

(3) Features are extracted from the wavelet coefficients of the measured cutting force and simulated cutting force. Suitable features are those that are sensitive to tool wear when ball-nose end milling sculptured surface.

(4) Neural network applications are proposed to map the features (input) to tool wear level (output) by training via examples. Support vector machines for regression (SVR) is employed in this work. In order to perform tool wear estimation, SVR is trained by a training data set. Pairs of feature vector and tool wear value form the training data set.

3.3 Cutting force simulation using discrete mechanistic cutting force model

3.3.1 Mechanistic model

Lee and Altintas (1996) suggested that the resultant milling force can be resolved into a cutting force component and a ploughing force component to more accurately predict the cutting forces. The cutting force component is the force required to remove the chip. The ploughing force is the force acting on the tool edge and tool flank face (tool-workpiece interface region). The instantaneous milling force at a particular rotation angle ϕ is:

$$dF(\phi, z) = K_e \cdot dS + K_c \cdot t(\phi) \cdot db \tag{3.1}$$

where dF is the elemental cutting forces, dS is the differential length of the curved cutting edge segment, $t(\phi)$ is the undeformed chip thickness normal to the cutting edge, db is the chip width in each cutting edge discrete element.

In this model, K_e is the ploughing force coefficient, K_c is the shearing coefficients. As "size effect" has been represented by ploughing force component, K_c does not vary with chip thickness. The calibration process is simplified significantly by this assumption.

The discrete cutting force models are developed by slicing the cutter into a series of axial discs. Each flute of the tool is divided into a few elemental cutting edges and the cutting force is summed up from each elemental cutting edge. From geometrical point of view, the milling operation on each elemental cutting edge is oblique cutting; so the cutting force on the elemental cutting edge can be considered as a resultant force of three force components. The three force components are differential cutting forces in tangential, radial and axial direction, and can be expressed as a function of cutter rotation angle and axial position.

$$\begin{cases} dF_t = K_{te} \cdot dS(z) + K_{tc} \cdot t(\varphi) \cdot db \\ dF_r = K_{re} \cdot dS(z) + K_{rc} \cdot t(\varphi) \cdot db \\ dF_a = K_{ae} \cdot dS(z) + K_{ac} \cdot t(\varphi) \cdot db \end{cases} \tag{3.2}$$

where F_t, F_r, F_a are elemental tangential, radial, and axial cutting forces, (K_{te}, K_{re}, K_{ae}) are edge force coefficients, (K_{tc}, K_{rc}, K_{ac}) are shearing coefficients, dS is the differential length of the curved cutting edge segment, $t(\phi)$ is the undeformed chip thickness normal to the cutting edge, db is the chip width in each cutting edge discrete element.

The assumption in this model is that the individual movement of the cutter is at a constant orientation. For 3-axis milling case, this can be represented by a constant tilted surface on the workpiece. This assumption is based on the reality that the typical orientation change between individual movements is small and continuous.

The differential length of the curved cutting edge segment can be calculated from the geometric model of a ball-end mill. Assume that the helical ball-end milling cutter is ground with a constant helix lead and a point P located on the helical flute has Cartesian coordinate (x, y, z). If the helix angle of the flutes at the ball-shank meeting boundary is β_0, the lag angle ψ between the tool tip (z=0) and point P is
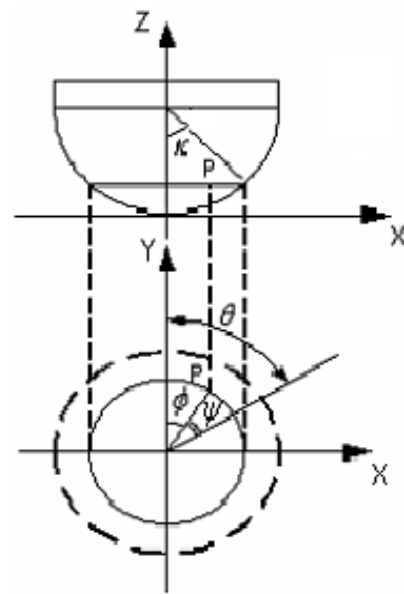
Figure 3.2 Ball-nose end mill geometry

$$\psi = \frac{z \cdot \tan(\beta_0)}{R_0}$$

(3.3)

Let θ be the rotation angle at tool tip, the instantaneous angle of immersion of the given disc is

$$\phi = \theta - \psi$$

(3.4)

therefore, if the number of teeth of the tool is *n*, the instantaneous angle of immersion of *ith* tooth is

$$\phi_i(\theta, z) = \theta - \frac{z}{R_0} \tan \beta_0 - (i - 1) \frac{2\pi}{n}$$

(3.5)

On the other hand, $P(x, y, z)$ can be associated to a spherical coordinate (R_0, κ, ϕ), where R_0 is the ball radius of the cutter, κ is measured from the $-z$ axis, and ϕ is measured clockwise from the $+y$ axis. κ is calculated as follows,

$$\kappa = \arccos\left(\frac{R_0 - z}{R_0}\right) \text{ where } 0 \leq z \leq R_0 \tag{3.6}$$

The undeformed chip thickness is essential to the cutting force model. When the cutting edges engaged with the workpiece, the undeformed chip geometry can be determined by the feed per tooth and the tool geometry (Lamikiz et al., 2004).

In milling operation a CNC program controls the motion profile of the tool centre; in the mean time, the points on the cutting edges rotate about the centre of the spindle. According to Kaczmarek (1976), the shape of the tooth path in relation to the workpiece, which is a composition of the rotary motion of the cutter and the feed motion, is a trochoid. However, in most actual ball-end milling operations, when the cutting speed is much larger than the tool moving speed, the tool is assumed to follow a circular tooth path. Based on this assumption and the ball-end mill geometric model, the instantaneous undeformed chip thickness $t(\phi)$ and the chip width db can be determined as follows:

$$t(\phi) = f_t \cdot \sin(\phi) \cdot \sin(\kappa) \tag{3.7}$$

where f_t is the feed rate (mm/rev-tooth), ϕ is the instantaneous angle of immersion, κ is the angle between a point on the flute and the z-axis in the vertical plane.

$$db = \frac{dz}{\sin(\kappa)} \tag{3.8}$$

where κ is the angle between a point on the flute and the z-axis in the vertical plane, dz is the thickness of each disc.

The resultant forces in Cartesian coordinates are

$$\begin{bmatrix} dF_x \\ dF_y \\ dF_z \end{bmatrix} = \begin{bmatrix} -\sin(\kappa)\sin(\phi) & -\cos(\phi) & -\cos(\kappa)\sin(\phi) \\ -\sin(\kappa)\cos(\phi) & \sin(\phi) & -\cos(\kappa)\cos(\phi) \\ \cos(\kappa) & 0 & -\sin(\kappa) \end{bmatrix} \begin{bmatrix} dF_r \\ dF_t \\ dF_a \end{bmatrix} \tag{3.9}$$

The total cutting forces acting on one flute j is

$$F_{xj} = \int_{z_1}^{z_2} (-dF_{rj}\sin(\kappa_j)\sin(\phi_j) - dF_{tj}\cos(\phi_j) - dF_{aj}\cos(\kappa_j)\sin(\phi_j))dz \tag{3.10}$$

$$F_{yj} = \int_{z_1}^{z_2} (-dF_{rj}\sin(\kappa_j)\cos(\phi_j) + dF_{tj}\sin(\phi_j) - dF_{aj}\cos(\kappa_j)\cos(\phi_j))dz \tag{3.11}$$

$$F_{zj} = \int_{z_1}^{z_2} (dF_{rj}\cos(\kappa_j) - dF_{aj}\sin(\kappa_j))dz \tag{3.12}$$

3.3.2 Model building using average force

In ball-end milling, the cutter edge length changes according to the local helix angle. If the tool is sliced into small discs with constant height along the Z-axis, the length of the cutter edge increases rapidly as the Z-axis position of the disc element approaches zero, consequently, the contact area of the flank face with the workpiece increases accordingly. In the case of horizontal slot machining on horizontal surface, the ploughing force increases as the Z-axis position approaches the bottom disc. To avoid edge rubbing at the bottom disc of the ball-end mill, an inclined surface was used to build the cutting force model.

As the cutter travels along the path on the sculptured surface, chip thickness and cutting force direction varies with the changes of the intersection of the cutter and the workpiece, while the cutting force magnitude varies with the change in the chip load. In order to predict the chip load and the cutting forces, the entry angle ϕ_{st} and the exit

angle ϕ_{ex}, which change continuously, are evaluated from the geometric intersection of the cutter and the workpiece. The engagement conditions (ϕ_{st}, ϕ_{ex}) lead to the prediction of varying chip thickness at each tool location as it rotates. Cutter and workpiece intersection boundaries along the tool path must be identified for the prediction of cutting forces.

It is desired to determine ball-nose end milling cutting force model coefficients by using fundamental orthogonal cutting parameters if those parameters are available in a data base. However, in some practical cases, it may not be possible to create a time-consuming orthogonal cutting data base to determine the calibration coefficients. Therefore, the mechanistic approach is still widely accepted as a quick method of calibrating the cutting force model (Lamikiz et al., 2004).

It is essential that a simple and non-invasive calibration method to be used when the models are used on the machine shop floor. There are two assumptions in the characterization tests. Firstly, edge coefficients which are related with friction can be considered as constant. Secondly, shear coefficients are dependent on Z axis. The approximation can be considered as linear coefficients and thus a Z-coordinate polynomial will be used to determine the axial calibration coefficient pattern.

For a particular workpiece-cutter combination, the average force data measured in a set of model building experiments are required to identify the numerical values of the model parameters. The average cutting force per tooth period is independent of the helix angle. The integration for the average force of the measured force is done in one revolution. In order to get the calculated force, the cutting force is integrated axially at each incremental rotation angle, from the bottom disc to the upper disc at axial depth of cut. By comparing the calculated equation with the experimental average cutting

force values, the cutting force model coefficients can be identified. The average forces expressions are computed in following numerical way.

As shown in Figure 3.3, let i be the index of the discs along the Z-axis direction, the disc locating angle at i-th disc $\kappa(i)$ is the angle between a point on the flute and the Z-axis in the vertical plane. At the sphere part, the discs are
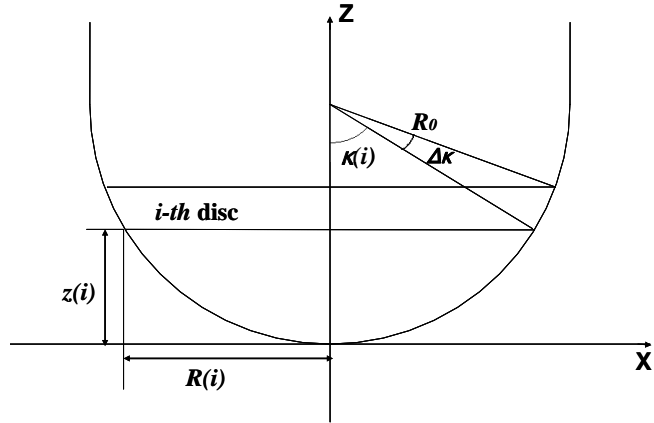
Figure 3.3 Discrete cutting edges

sliced uniformly in the locating angle; on the other hand, the thickness of each disc in Z-axis direction is not uniform.

Let $\Delta\kappa$ be the uniform slicing in the disc locating angle, the chip width at each disc is

$$\Delta b = R_0 \cdot \Delta\kappa \tag{3.13}$$

where R_0 is the radius of the ball.

At i-th disc, the relation between the Z-axis coordinate $z(i)$ and the locating angle $\kappa(i)$ $(0 \le \kappa(i) \le \pi/2)$ is

$$z(i) = R_0 \cdot (1 - \cos\kappa(i)) \tag{3.14}$$

The local radius at i-th disc is

$$R(i) = \sqrt{R_0^{\,2} - (R_0 - z(i))^2} \tag{3.15}$$

The local helix angle at i-th disc is

$$\beta(i) = \arctan(\frac{R(i)}{R_0}\tan\beta_0) \tag{3.16}$$

where β_0 is the helix angle at flute and shank meeting point.

Therefore, the length of the cutting edge at *i-th* disc can be determined as

$$\Delta S(i) = \frac{R_0 \cdot \Delta \kappa}{\cos \beta(i)} \tag{3.17}$$

As shown in Figure 3.4, tool rotation angle θ is measured clock wise from +y-axis.

Due to the helix angle, the lag angle between the flute at *i-th* disc and tool tip is

$$\psi(i) = \frac{z(i)}{R_0} \tan \beta_0 \tag{3.18}$$

Let *j* be the index of the tool rotation angle, when the tool rotation angle is $\theta(j)$, the instantaneous angle of immersion at *i-th* disc is:

$$\phi(i, j) = \theta(j) - \psi(i) \tag{3.19}$$

Hence when the tool rotation angle is $\theta(j)$, the instantaneous undeformed chip thickness at *i-th* disc is

$$t(i, j) = f_t \cdot \sin \phi(i, j) \cdot \sin \kappa(i) \tag{3.20}$$

where f_t is the feed per tooth per revolution.
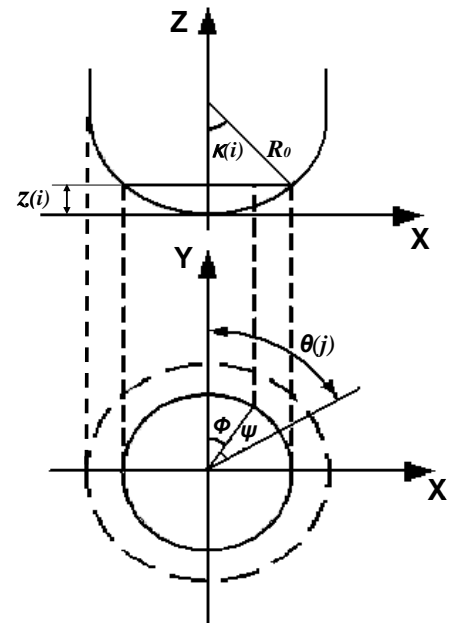
Figure 3.4 Tool rotation angles

When the tool rotation angle is $\theta(j)$, the cutting force at *i-th* disc can be expressed as follows:

$$F_t(i, j) = K_{te} \cdot \Delta S(i) + K_{tc} \cdot t(i, j) \cdot \Delta b \tag{3.21}$$

$$F_r(i, j) = K_{re} \cdot \Delta S(i) + K_{rc} \cdot t(i, j) \cdot \Delta b \tag{3.22}$$

$$F_a(i, j) = K_{ae} \cdot \Delta S(i) + K_{ac} \cdot t(i, j) \cdot \Delta b \tag{3.23}$$

The average cutting force per tooth period can be expressed as follows:

$$\bar{F}_x = \frac{1}{n_\theta} \sum_{j=1}^{n_\theta} \sum_{i=1}^{n_z} (-F_r(i,j)\sin\kappa(i)\sin\phi(i,j) - F_t(i,j)\cos\phi(i,j) - F_a(i,j)\cos\kappa(i)\sin\phi(i,j))$$

(3.24)

$$\bar{F}_y = \frac{1}{n_\theta} \sum_{j=1}^{n_\theta} \sum_{i=1}^{n_z} (-F_r(i,j)\sin\kappa(i)\cos\phi(i,j) + F_t(i,j)\sin\phi(i,j) - F_a(i,j)\cos\kappa(i)\cos\phi(i,j))$$

(3.25)

$$\bar{F}_z = \frac{1}{n_\theta} \sum_{j=1}^{n_\theta} \sum_{i=1}^{n_z} (F_r(i,j)\cos\kappa(i) - F_a(i,j)\sin\kappa(i))$$

(3.26)

In order to determine the engagement of the cutting, the overlapping of previous cut portion for subsequent pass need to be modelled (Subrahmanyam et al., 2007). The engagement area is divided into two areas to calculate the entry angle and exit angle.
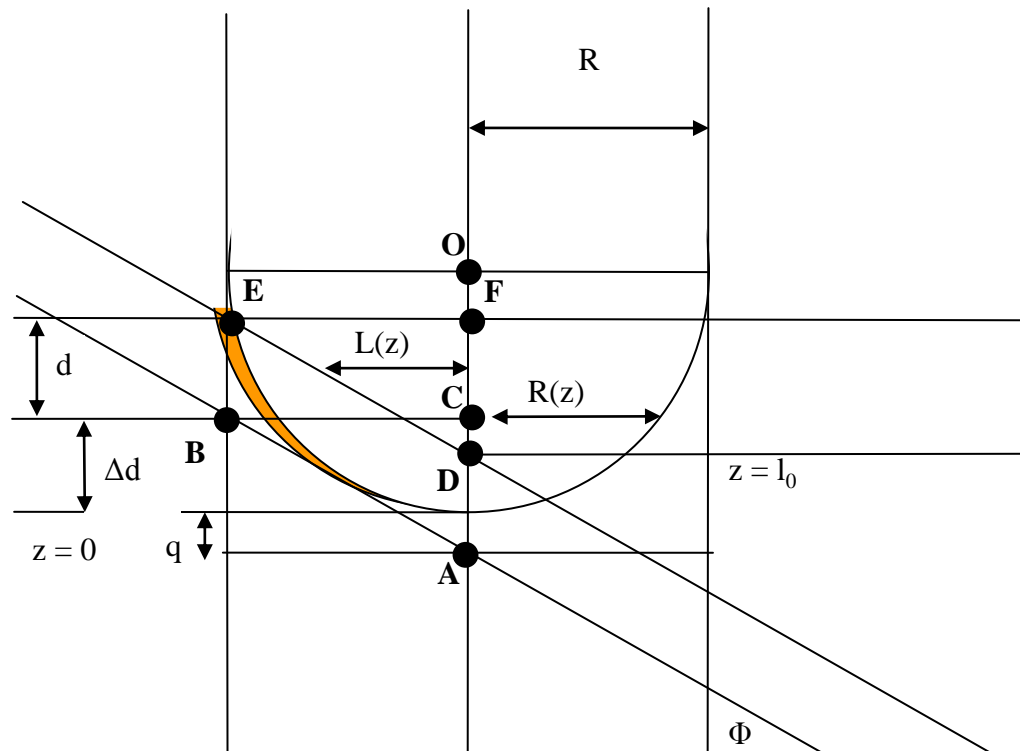
Figure 3.5 Determine the boundary of integration

In order to simulate the cutting force, the entry angle and exit angle need to be determined. In Figure 3.5, the material is slanted by Φ degrees, and the highlighted area is the material to be removed. From this figure, $L(z)$ is the shortest distance between the plane that pass through the spindle axis with normal line directed to the right and the material.

In triangle ABC,

$$\overline{AC} = R \tan \phi \tag{3.27}$$

$$k = \overline{OA} - R = R\left(\frac{1 - \cos \phi}{\cos \phi}\right) \tag{3.28}$$

Hence

$$\Delta d = p - q = R\left(\frac{\sin \phi + \cos \phi - 1}{\cos \phi}\right) \tag{3.29}$$

Using congruency between triangle DEF and the triangle created from the $L(z)$ line and point D, $L(z)$ can be calculated as

$$L(z) = R\,\frac{z - l_0}{(d + \Delta d) - l_0} \tag{3.30}$$

$$l_0 = d + \Delta d - R \tan \phi \tag{3.31}$$

Using this value, the enter and exit angle can be calculated as

$$\theta_{enter} = \arcsin \frac{L(z)}{R(z)} \tag{3.32}$$

$$\theta_{exit} = 180 - \theta_{enter} \tag{3.33}$$

Note that $L(z) = 0$ if $z < l_0$

3.3.3 Experimental verification

<u>Workpiece material, cutting tool and equipment</u>

The experiments were conducted on a 3-axis milling machine as shown in Figure 3.6.
The workpiece material was hardened Stavax mould steel and the hardness is 45 HRc.
10mm insert based carbide ball nose end mills with $30°$ helix angle were used in the
experiments. The cutting force was measured by a Kistler quartz 3-component
platform dynamometer. The dynamometer was mounted between the workpiece and
machining table as shown in Figure 3.7. The cutting forces in the X, Y and Z
directions were sampled by PC208AX Sony data recorder as shown in Figure 3.8.

Figure 3.6 Milling machine for experiments

Figure 3.7 Dynamometer and workpiece
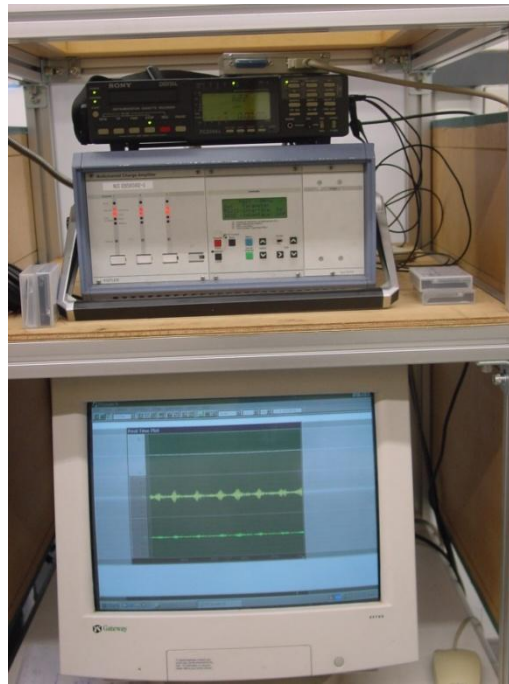
Figure 3.8 Data acquisition system

<u>**Experimental parameters and procedure**</u>

The model building experiments involved horizontal slot milling on a $45\,°$ inclined surface. Twenty eight cutting tests were conducted on a 3-axis milling machine with feed per tooth from 0.05 mm to 0.2 mm and the depth of cut from 0.2 mm to 0.5 mm.

<u>**Verification results**</u>

The cutting force model has been validated by comparing the simulated and the measured cutting forces. The cutting force can be estimated using the cutting force model for given cutting conditions. The results are shown in Figure 3.9. From the figure, the simulated cutting forces are in very close agreement with the measured cutting forces in cutting force waveform. The estimated tool entry and exit angle from the model are quite near to experimental data, that means the engagement and disengagement of the tool with workpiece was closely matched with the experimental result.
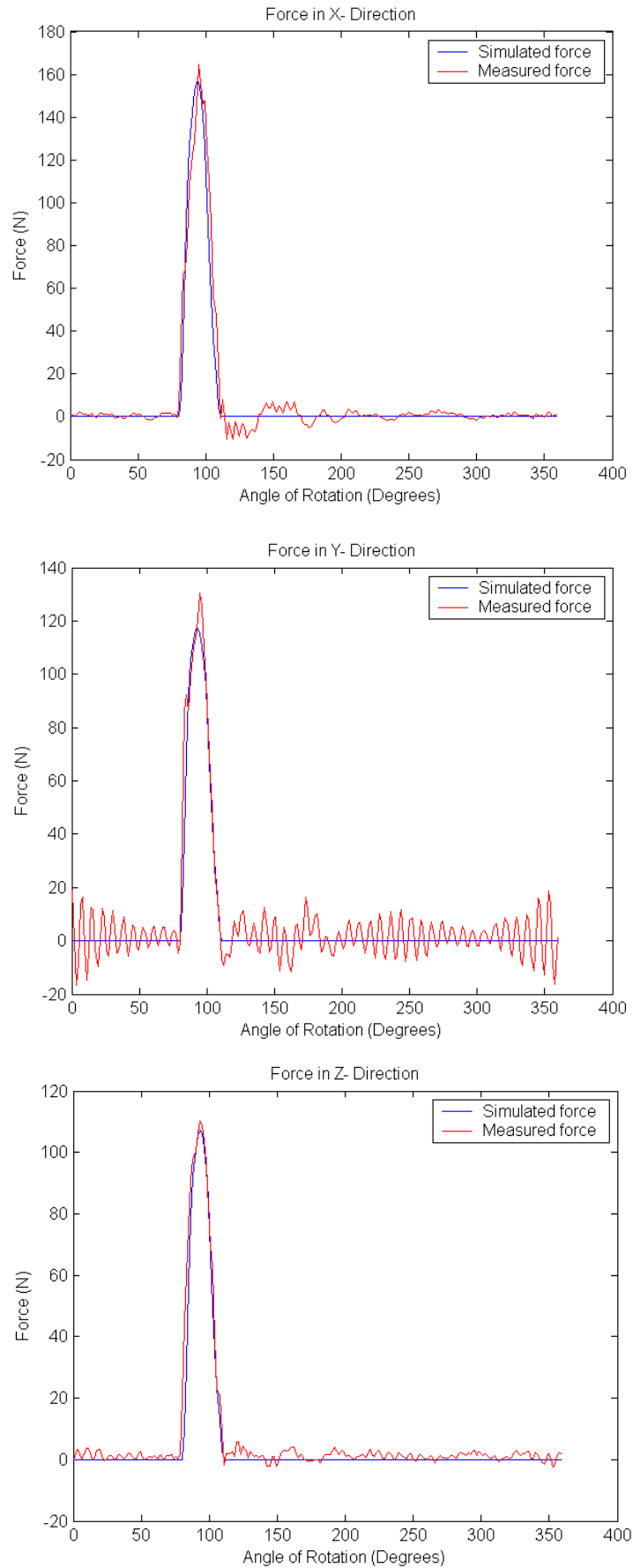
**Figure 3.9 Simulated and measured cutting force
(DOC = 0.2 mm, feedrate = 0.2 mm/tooth/rev)**

The comparison of the mean and maximum force of cutting force model with that of the experimental data is a way to validate the model (Subrahmanyam, 2009). The mean and maximum force features are calculated in one revolution rotation of the cutter. The mean cutting force is calculated as the mean force within tool entry angle and exit angle in one revolution. The ensemble average of the maximum force and mean force from fresh tool cutting experimental data are calculated as force features. In this experiment, the error was less than 10% in average. Kapoor et al. (1998) and Lazoglu and Liang (2000) suggested that the reasonable accuracy of the developed cutting force models is within 15% in average. From these results it can be said that the experimentally determined cutting force model coefficients are acceptable.

3.4 Discrete wavelet analysis of cutting force sensor signal

The continuous wavelet transformation is expressed as follows (Wang and Gao, 2006):

$$C(a,b) = \int_R s(t) \frac{1}{\sqrt{a}} \psi\left(\frac{t-b}{a}\right) dt, \ a \in R^+ - \{0\}, \ b \in R \qquad (3.34)$$

where $s(t)$ is the signal, $\frac{1}{\sqrt{a}} \psi\left(\frac{t-b}{a}\right)$ is wavelet function, a is scale factor, b is shifting factor.

In wavelet analysis, the scaling function ϕ and the wavelet ψ generate a family of functions that can be used to break up or reconstruct a signal. If $s(t)$ represents a cutting force signal in a finite time window $[-t_0, t_0]$, when shifting factor is fixed, $C(a, b)$ depends on $s(t)$ in the time interval $[b-at_0, b+at_0]$. So decreasing scale factor will make the time interval shorter and gives better localization in the time domain.

Therefore, the adaptive window width in wavelet transform is an advantage for analyzing and monitoring the rapid transient of small amplitude of cutting force signal when cutting engagement changes along the sculptured surface tool path.

The detailed discrete wavelet analysis (Hong et al., 1996) is described as follows:

Assuming Vj is a multi-resolution approximation, ϕ and ψ are scaling function and orthogonal wavelet, respectively, and original signal $f(x)$ is measurable and has a finite energy: $f(x) \in V_{J_1}$ then $f(x)$ can be decomposed:

$$f(x) = A_{J_1} = A_{J_1+1} f(x) + D_{J_1+1} f(x) \tag{3.35}$$

where

$$A_{J_1+1} f(x) = \sum_{m=-\infty}^{+\infty} C_{J_1+1,m} \phi_{J_1+1,m} \tag{3.36}$$

$$D_{J_1+1} f(x) = \sum_{m=-\infty}^{+\infty} D_{J_1+1,m} \psi_{J_1+1,m} \tag{3.37}$$

$$C_{J_1+1,m} = \sum_{k=-\infty}^{+\infty} \overline{h}_{k-2m} C_{J_1,k} \tag{3.38}$$

$$D_{J_1+1,m} = \sum_{k=-\infty}^{+\infty} \overline{g}_{k-2m} C_{J_1,k} \tag{3.39}$$

and the inner product

$$\langle \phi_{J_1,k}, \phi_{J_1+1,m} \rangle = \overline{h}_{k-2m} \tag{3.40}$$

$$\langle \phi_{J_1,k}, \psi_{J_1+1,m} \rangle = \overline{g}_{k-2m} \tag{3.41}$$

Let $H = [\overline{h}_{k-2m}]$, $G = [\overline{g}_{k-2m}]$ then

$$C_{J_1+1} = HC_{J_1} \tag{3.42}$$

$$D_{J_1+1} = GC_{J_1} \tag{3.43}$$

By repetitively decomposing $A_{J_1+1}f(x)$ for J_2 times,

$$f(x) = A_{J_2}f(x) + \sum_{j=J_1+1}^{J_2} D_j f(x) \tag{3.44}$$

where

$$A_j f(x) = \sum_{k=-\infty}^{+\infty} C_{j,k}\phi_{j,k}(x) \tag{3.45}$$

$$D_j f(x) = \sum_{k=-\infty}^{+\infty} D_{j,k}\psi_{j,k} \tag{3.46}$$

$$C_{j+1} = HC_j \tag{3.47}$$

$$D_{j+1} = GC_j \tag{3.48}$$

$(j = J_1, J_1+1 ... J_2-1)$

According to Mallat pyramidal algorithm, original signal $f(x)$ can be decomposed to different frequency bands by discrete approximation component and discrete detail components. Wavelet analysis can be considered as a series of band pass filters. It extracts information from the original signal $f(x)$ by decomposing it into a series of approximations A and details D distributed over different frequency bands. Given the sampling frequency fs, the frequency of the signal $f(x)$ is 0.5 fs. The bandwidths of the approximation A and detail D at the level l are $\left[0, \frac{1}{2}f_s 2^{-l}\right]$, $\left[\frac{1}{2}f_s 2^{-l}, \frac{1}{2}f_s 2^{-(l-1)}\right]$ respectively.

Since Daubechies wavelets perform well in separating the frequency bands during signal decomposition, they are selected for feature extraction in this research.

3.5 Tool wear monitoring from cutting force feature

3.5.1 Feature extraction

In order to maximize the information utilization of cutting force signals, features are extracted from the wavelet coefficients. Tool wear states are reflected by the varied characteristics of the extracted features (Sun et al., 2006). According to the observation by Choi et al. (2004), the approximations in wavelet coefficients will reflect tool wear in end milling processing. After the signal is decomposed through wavelet transform, the signal energy is represented by the approximation coefficients.

To obtain feature vectors from the cutting force model, the measured and simulated cutting force are processed through wavelet transform. The residual difference between the measured and simulated approximation coefficients can be a sensitive feature vector, which is used for the evaluation of the difference between measured force and simulated force. When the tool is in good condition, this measure has the lower value which shows the force signals are well matched. Three kinds of residual measurements are used in this work:

Residual Maximum Approximation Coefficients (RMA):

$$RMA = (\max(A_m) - \max(A_s)) / \max(A_s) \qquad (3.49)$$

Residual Average Approximation Coefficients (RAA):

$$RAA = (\bar{A}_m - \bar{A}_s) / \bar{A}_s \qquad (3.50)$$

Average Residual Energy (ARE):

$$ARE = \frac{1}{N} \sum_{i=1}^{N} ((A_m(i))^2 - (A_s(i))^2) \qquad (3.51)$$

where $A_m(\ i\ )$ and $A_s(\ i\ )$ are wavelet approximation coefficients from measured cutting force and simulated cutting force respectively, N is the total number of wavelet coefficients.

The feature evaluation method in this work is to select those which give high correlation with the observed tool wear. As those features are not equally informative, the correlation coefficient is used to identify suitable features for tool wear estimation.

Correlation coefficients between the feature (x) and measured flank wear (y) is calculated as

$$R_{xy} = \frac{\mathrm{cov}(x, y)}{[\mathrm{var}(x)\,\mathrm{var}(y)]^{1/2}} \tag{3.52}$$

where cov(x, y) is the covariance between wear and the feature, var(x) and var(y) are the variance of x and y. The covariance function cov(x, y) is defined as

$$\mathrm{cov}(x, y) = E[(x - E[x])(y - E[y])] \tag{3.53}$$

where E is the mathematical expectation.

The performances of the features are evaluated by correlation coefficients. This statistical method is a normalized measure of the strength of the relationship between the feature and tool wear. If certain feature corresponds to noise, not relevant to the tool wear process, the correlation coefficient will be small (i.e. uncorrelated data results in a correlation coefficient of 0). Features correlated to tool wear will have high correlation coefficient (≥ 0.8).

3.5.2 Tool wear estimation using support vector machines for regression (SVR)

By training through examples, a machine learning method can be used to map suitable features (input) derived from the cutting force to the tool wear level (output). Among the machine learning methods, support vector regression (SVR) is a new generation of machine learning algorithm which was developed by Vapnik et al (Vapnik, 1995). It is a well-established universal approximator of any multivariate function (Haykin, 1999). Consequently, as a supervised method, SVR has been selected to establish the non-linear relation between the cutting force and tool wear, taking advantage of prior knowledge of the tool wear. Therefore, in this work a nonlinear regressive model is proposed to describe the dependence of flank wear (*VB*) on cutting force feature vector (**x**):

$$VB = f(\mathbf{x}) + v \tag{3.54}$$

where v is noise term which is independent of feature vector **x**.

For a given set of training data $\{(\mathbf{x}_i, d_i)\}_{i=1}^{N}$, where $\mathbf{x}_i \in R^m$ is a sample value of the input feature vector **x** and di is the corresponding tool wear value in model output *VB*. Support vector machines for regression (SVR) is to provide an estimate of the dependence of *VB* on **x** (Haykin, 1999):

$$VB_e = \sum_{j=0}^{m_1} w_j \varphi_j(\mathbf{x}) = \mathbf{w}^T \varphi(\mathbf{x}) \tag{3.55}$$

where *w* is the weight vector, $\varphi(\mathbf{x})$ denotes a set of non-linear transformation from the input space into the feature space of dimension m_1.

The estimate is constructed to minimize the cost function:

$$\Phi(\mathbf{w}, \xi, \xi') = C \left(\sum_{i=1}^{N} (\xi_i + \xi'_i) \right) + \frac{1}{2} \mathbf{w}^T \mathbf{w} \qquad (3.56)$$

Subject to the constraints:

$$d_i - \mathbf{w}^T \varphi(\mathbf{x}_i) \leq \varepsilon + \xi_i, \qquad i = 1,2,..., N$$

$$\mathbf{w}^T \varphi(\mathbf{x}_i) - d_i \geq \varepsilon + \xi'_i, \qquad i = 1,2,..., N$$

$$\xi_i \geq 0, \qquad i = 1,2,..., N$$

$$\xi'_i \geq 0, \qquad i = 1,2,..., N$$

where $\{\xi_i\}_{i=1}^{N}$ and $\{\xi'_i\}_{i=1}^{N}$ are two sets of slack variables.

Using the method of Lagrange multipliers, one may now state the dual problem for nonlinear regression using a support vector machine as follows:

Given the training sample $\{(\mathbf{x}_i, d_i)\}_{i=1}^{N}$, find the Lagrange multipliers $\{\alpha_i\}_{i=1}^{N}$ and $\{\alpha'_i\}_{i=1}^{N}$ that maximize the objective function

$$Q(\alpha_i, \alpha'_i) = \sum_{i=1}^{N} d_i(\alpha_i - \alpha'_i) - \varepsilon \sum_{i=1}^{N} (\alpha_i + \alpha'_i) - \frac{1}{2} \sum_{i=1}^{N} \sum_{j=1}^{N} (\alpha_i - \alpha'_i)(\alpha_j - \alpha'_j) K(\mathbf{x}_i, \mathbf{x}_j) \qquad (3.57)$$

subject to the following constraints:

(1) $\sum_{i=1}^{N} (\alpha_i - \alpha'_i) = 0$

(2) $0 \leq \alpha_i \leq C, \qquad i = 1,2,..., N$

$\quad\ 0 \leq \alpha'_i \leq C, \qquad i = 1,2,..., N$

where C is a user-specified constant.

In the training phase, training datasets are used to build SVR model for the estimation of the tool wear. Firstly, the training datasets are used to tune the model parameters by k-fold cross validation method. Secondly, the training datasets are used to obtain

the weights of the estimation function by optimization algorithm. After the SVR model has been built, the regression accuracy can be tested by the test datasets.

3.6 Preliminary experimental results and discussion

3.6.1 Experimental set-up

To analyze the influence of wear on the cutting force in ball-nose end milling applications, ball-nose end milling was performed on an inclined surface (Klocke et al., 2000). The presented experiments will focus on milling an inclined surface with a fixed angle at different depth of cut and cutting speed.

Workpiece material, cutting tool and equipment

The experiments were conducted on a 3-axis milling machine. The workpiece material was hardened Stavax mould steel and the hardness is 45 HRc. 10mm insert based carbide ball nose end mills with
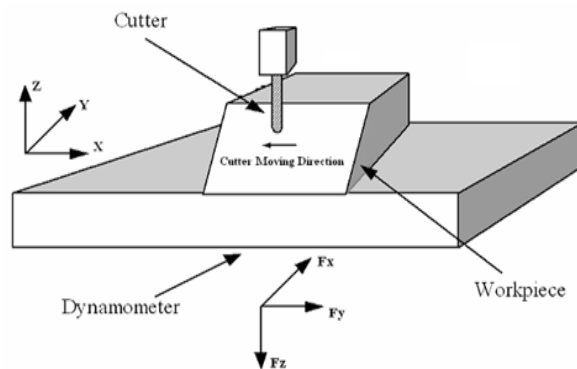
Figure 3.10 Ball-nose end milling an inclined surface

$30°$ helix angle were used in the experiments. The cutting force was measured by a Kistler quartz 3-component platform dynamometer. The dynamometer was mounted between the workpiece and machining table. The cutting forces in the X, Y and Z directions were sampled by PC208AX Sony data recorder. The tool wear was measured by Olympus microscope.

Experimental parameters and procedure

The milling process in the experiments is to create an oblique plane surface on a workpiece by ball-nose end milling operation. The geometric form is created by means of the tool path, not the cutter shape.

The target of this experiment is to mill a 45 °inclined surface. The tool moves forward to create one horizontal cut on the inclined surface. The horizontal cuts were repeated at fixed pitch and depth of cut. The experiments were performed at different feed rate, depth of cut, and spindle speed. The tool wear was measured at a fixed interval. Then the cutting was repeated again until the severe tool wear happened. The cutting forces in the X, Y and Z directions were sampled with 3,000Hz sampling rate.

3.6.2 Energy distributions of cutting force

As introduced in previous sections, the inputs of SVR model are feature vectors extracted from cutting force data. Feature extractions are conducted based on the discrete wavelet transform (DWT) techniques. To determine the useful frequency band of the decomposed data for feature extraction, energy distribution using DWT was evaluated. After the cutting force data are decomposed by DWT, the energy distribution can be described by Parseval's theorem (Gaing, 2004):

$$\frac{1}{N}\sum_{t}\left|f(t)\right|^{2} = \frac{1}{N_{J}}\sum_{k}\left|cA_{J,k}\right|^{2} + \sum_{j=1}^{J}\left(\frac{1}{N_{j}}\sum_{k}\left|cD_{j,k}\right|^{2}\right) \qquad (3.58)$$

Figure 3.11 shows the wavelet energy distributions of cutting force in X, Y and Z direction. As the sampling rate was 3000Hz in this experiment, the cutting force data were decomposed into the constituent parts at frequency bands A6: [1 Hz, 23 Hz], D6:

[24 Hz, 46 Hz], D5: [47 Hz, 93 Hz], D4: [94 Hz, 187 Hz], D3: [188 Hz, 375 Hz], D2: [376 Hz, 750 Hz], D1: [751 Hz, 1500 Hz]. The result showed that the energy level of the low frequency band (1-375Hz) was much higher than that of middle and high frequency band. This result is probably due to the fact that the energy of cutting force tends to be concentrated at tooth passing frequency and its low frequency harmonics.
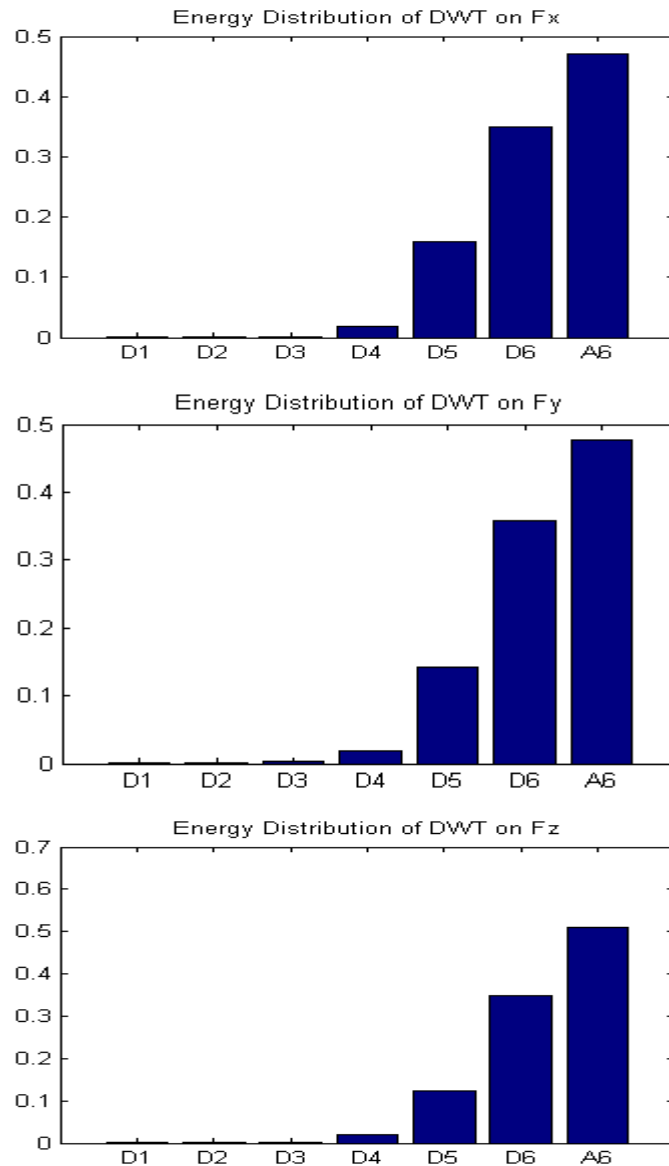
Figure 3.11 Energy distributions of cutting force in X, Y and Z direction

Based on this result, the wavelet transformation was repeated twice to obtain the coefficients in subsequent experiments. Through wavelet transformation, the

experimental cutting force data were decomposed into the constituent parts at frequency bands [1 Hz, 375 Hz], [376 Hz, 750 Hz] and [751 Hz, 1500 Hz], respectively. In this way, cutting force data in low frequency band (1-375Hz) were extracted for feature extraction. In this study, the residual between wavelet approximations of the simulated force data and wavelet approximations of measured force data were used for feature extraction.

3.6.3 Feature extraction

Table 3.1 shows the features that are used as inputs of SVR to monitor the tool wear. The features are energy related features based on the cutting force model. These features have been evaluated by correlation coefficients. As cutting force components are measured in X, Y and Z direction, a total of nine features are used to train and test the SVR model.

Table 3.1 Features for tool wear estimation

Index	Definition
X1	Residual Maximum Approximation Coefficients at X direction (RMA_X)
X2	Residual Maximum Approximation Coefficients at Y direction (RMA_Y)
X3	Residual Maximum Approximation Coefficients at Z direction (RMA_Z)
X4	Residual Average Approximation Coefficients at X direction (RAA_X)
X5	Residual Average Approximation Coefficients at Y direction (RAA_Y)
X6	Residual Average Approximation Coefficients at Z direction (RAA_Z)
X7	Average Residual Energy at X direction (ARE_X)
X8	Average Residual Energy at Y direction (ARE_Y)
X9	Average Residual Energy at Z direction (ARE_Z)

In the objective function (3.57), $K(\mathbf{x}_i, \mathbf{x}_j)$ is the kernel function. It is to map the feature data from the original space into the high dimensional space (Sun et al., 2004a). In this work, Gaussian kernel is chosen as the kernel function:

$$K(\mathbf{x}_i, \mathbf{x}_j) = \exp\left(-\frac{\|\mathbf{x}_i - \mathbf{x}_j\|^2}{2\sigma^2}\right) \tag{3.59}$$

For different problem, the penalty parameter C, the error tolerance threshold ε and the value of σ from the kernel function have to be tuned to achieve good performance with SVR models. The optimum parameters for a given problem are found by grid search method using cross-validation (Duan et al., 2003).

The generalization error is estimated by using k-fold cross validation:

(1) Divide the training data set into k subsets (the folds) randomly. The subsets are mutually exclusive approximately equal size.

(2) Train the SVR using k-1 subsets.

(3) Test the SVR using the remaining 1 subset and obtain the error.

(4) Repeat (step 2 and step 3) k times to ensure that each subset has been used to test SVR once.

(5) Estimate the generalization error by averaging all the test errors over the k tests.

In this way, each data subset of the whole data set has been predicted once for calculating the generalization error. In this work, 5-fold cross-validation on the training set is used to find the optimum parameters. The prediction accuracies for cross-validation are compared in terms of the averaged absolute estimation error:

$$\frac{\sum_{i=1}^{N} \left| d_i - \mathbf{w}^T \varphi(\mathbf{x}_i) \right|}{N} \tag{3.60}$$

3.6.4 Tool wear estimation using support vector regression (SVR)

To construct the SVR model, the training data sets were obtained under various cutting parameters used in the experiment. The remaining data sets using different cutting parameters were used for testing. Table 3.2 shows the cutting conditions used in the experiments. In the experiments, a total of 60 measurement samples (22500 data in every sample) corresponding to various tool wear values were collected. Figure 3.12 shows a testing result of a tool wear estimation using the constructed SVR model. The result showed that the constructed SVR model performed well in this method, although the cutting conditions in the testing data set were not used in the training process. Therefore, this method has good performance in terms of generalization.
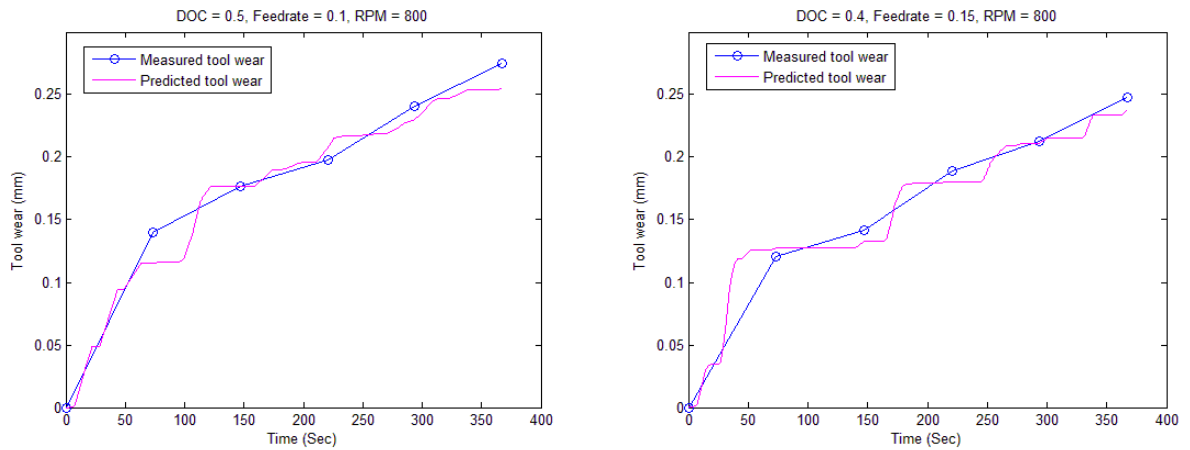
Figure 3.12 Comparison of the predicted tool wear and the measured tool wear

Table 3.2 Cutting conditions

Feed per tooth (mm/tooth/rev)	Depth of cut (mm)
0.050	0.4
0.075	0.4
0.100	0.4
0.125	0.4
0.150	0.4
0.050	0.5
0.075	0.5
0.100	0.5
0.125	0.5
0.150	0.5

3.7 Conclusion

A model-based tool wear estimation method is proposed to monitor ball-nose end milling process. Tool wear was monitored by capturing force signals on-line. As force signals were convoluted with noise from the milling process, cutting force signals were collected and processed using wavelet technique due to its adaptive window width.

A mechanistic cutting force model has been built, and the simulated cutting forces are used as reference to extract the residual features. The residual features have been explored to maximize the information utilization of force signals. These features are used as inputs of decision making module. Support vector machines for regression (SVR) are trained by the feature vectors to build a tool wear estimation model to on-line predict tool wear. The experimental results showed that the model based approach is feasible and effective.

Chapter 4

Further Study and Enhancement of Model-based Tool Wear Monitoring

4.1 Introduction

As described in previous chapters, the tool wear estimation method includes three parts: cutting force data acquisition; feature extraction; and tool wear estimation using the support vector machines for regression (SVR). In the feature extraction, the features are extracted from cutting force data and used as inputs of the SVR for tool wear estimation. These features are evaluated by its correlation to tool wear based on the resulting correlation coefficient to select those that are strongly correlated to the tool wear development. Some features will provide overlapping or redundant information. On the other hand, as the tool wear process is complex and not linear relationship with these features, there exist higher-order interactions between some features. Hence a proper feature selection process is necessary before the features are used as inputs of the support vector machines.

The target of feature selection is to identify effective features and remove conflicting, redundant and insignificant ones. The feature selection process consists of three major parts:

(1) Decide a selection criterion to determine whether one feature subset is 'better' than another;

(2) Systematic search of feature subsets;

(3) Decide a stopping criterion that indicates when the search may be terminated.

4.2 Problem formulation

The purpose of using rough set theory (RST) is to reduce attributes of the decision table which is the input of the SVR model. This is to prevent over fitting and save the training time for SVR modeling. Another advantage is to improve the performance by removing conflicting attributes. After the features are described by the decision table using rough set, exhaustive calculation algorithm can be used to reduce the dimension of feature space. Genetic algorithm is another alternative method to find redundant features.

4.3 Discernibility-based data analysis

To select the relevant features, several approaches have been taken to evaluate the features including automatic relevance determination (ARD) (Sun et al., 2004a), singular value decomposition (SVD) (Zhou et al., 2009), and rough set theory (RST) (Shen et al., 2000). RST is used in this study by using discernibility matrices to reduce the dimension of feature space.

Rough set theory (RST) is a data mining tool to explore the hidden patterns in the data set. It is based on equivalence relations in the classification of objects.

One of the main advantages of rough set data analysis is that it only uses information inside the training data set, that is, it does not rely on prior knowledge, such as prior probabilities. Feature selection using rough sets only focus on the granularity structure of the data. The fundamental knowledge on rough set theory (RST) is introduced in

this section following the notion of an information system presented in the works of Shen et al. (2000).

In rough set framework, knowledge (data) is represented by an information system. The information system S can be defined by a pair of non-empty finite set U and A, where U represents a set of objects in the information system and A represents a set of attributes to describe the object. Each object in set U is interpreted by the value of the decision attribute d.

Let $S = (U, A)$ be an information system, $U = \{u_1, \ldots, u_n\}$, $A = \{a_1, \ldots, a_m\}$.

A decision table can be constructed as a $n \times (m + 1)$ table: each row is one of the objects in $U = \{u_1, \ldots, u_n\}$, column 1 to m are labeled by attributes $A = \{a_1, \ldots, a_m\}$, column m+1 is the decision attribute d.

For any $i \in \{1, \ldots, m\}$ and $j \in \{1, \ldots, n\}$, the intersection of the j-th row and the i-th column is the value of the attribute a_i of object u_j, which is denoted as $a_i(u_j)$.

For example, Table 4.1 represents 4 objects $\{u_1, u_2, u_3, u_4\}$ with 5 attributes $\{a_1, a_2, a_3, a_4, a_5\}$

Table 4.1 Decision table

	Energy_x (a1)	Energy_y (a2)	Energy_z (a3)	Max_x (a4)	Max_y (a5)	Tool wear (d)
u1	1	0	2	1	0	0-0.1
u2	0	0	1	2	1	0.1-0.2
u3	2	0	2	1	0	0.1-0.2
u4	1	2	2	1	0	0.2-0.3

Indiscernibility

Let $S = (U, A)$ be an information system, an equivalence relation $IND(B)$:

$$IND(B) = \{(x, y) \in U^2 : \forall a \in B, a(x) = a(y)\} \qquad (4.1)$$

Lower and upper approximation

Let $S = (U, A)$ be an information system and let $B \subseteq A$ and $X \subseteq U$

then B-lower and B-upper approximation of X is defined respectively as follows:

$$\underline{B}X = \bigcup\{Y \in U \,/\, IND(B) : Y \subseteq X\} \qquad (4.2)$$

$$\overline{B}X = \bigcup\{Y \in U \,/\, IND(B) : Y \cap X \neq \varnothing\} \qquad (4.3)$$

Discernibility matrix

A discernibility matrix can be constructed based on the decision table. Each element $c_{jk} \subseteq A$ consists of a set of attributes that can be used to discern between object u_j and u_k.

$$c_{jk} = \left\{a \in A : a(u_j) \neq a(u_k)\right\} \quad \text{for } j, k = 1, 2, \cdots n \qquad (4.4)$$

where $a(u_j)$ and $a(u_k)$ denote the value of the attribute of object u_j and u_k respectively.

$$c_{jk} = c_{kj} \qquad (4.5)$$

$$c_{jj} = 0 \qquad (4.6)$$

If there are identical or contradicted object in the table, even all the features cannot distinguish the objects. As the decision table is generated during feature extraction process, it is easy to make sure that there is no identical or contradicted object in the table. Therefore, the problem of feature selection is as follows:

For a given decision table T, the elements of its discernibility matrix meet the condition: $c_{jk} > 0$.

4.4 Feature selection using rough set theory (RST)

To use rough sets for feature selection, relevant features are searched for the object classification. Based on a set of reducts for a data set, some criteria for feature selection can be formed, for example, selecting features from a minimal reduct, i.e., a reduct containing minimal set of attributes (Swiniarski and Skowron, 2003). The research problem is on the development of an effective algorithm based on RST to reduce cutting force data or reduce non-relevant features. The definition is as follows:

Let $R \subset A$, $0 \leq \varepsilon < 1$ a real number, *P* is a set of pairs (u_j, u_k). Attributes from *R* separate at least $(1 - \varepsilon)|P|$ pairs from *P*.

4.5 Experimental results and discussion

Experimental set-up is introduced in Section 3.6. To determine whether RST can be used as a proper feature selection process, the original feature combination is reduced to a few different combinations of features by RST. Those combinations of features selected by RST were tested as input of SVR to estimate tool wear.

Table 4.2 lists all the possible features corresponding to tool wear. Nine features, $\{RMA\_X, RMA\_Y, RMA\_Z, RAA\_X, RAA\_Y, RAA\_Z, ARE\_X, ARE\_Y, ARE\_Z\}$ were used as original feature combination as input of SVR after normalization.

Table 4.2 Feature set that includes all the candidate features

Index	Definition
X1	Residual Maximum Approximation Coefficients at X direction (RMA_X)
X2	Residual Maximum Approximation Coefficients at Y direction (RMA_Y)
X3	Residual Maximum Approximation Coefficients at Z direction (RMA_Z)
X4	Residual Average Approximation Coefficients at X direction (RAA_X)
X5	Residual Average Approximation Coefficients at Y direction (RAA_Y)
X6	Residual Average Approximation Coefficients at Z direction (RAA_Z)
X7	Average Residual Energy at X direction (ARE_X)
X8	Average Residual Energy at Y direction (ARE_Y)
X9	Average Residual Energy at Z direction (ARE_Z)

In order to use rough set theory, all the feature data need to be discretized before the feature selection process. Table 4.3 shows the sample features, and Table 4.4 shows the corresponding discretized features.

Table 4.3 Sample features before discretization

RMA_X	RMA_Y	RMA_Z	RAA_X	RAA_Y	RAA_Z	ARE_X	ARE_Y	ARE_Z	Wear
0.235	0.271	0.316	0.259	0.215	0.329	0.393	0.381	0.559	0.084
0.269	0.262	0.454	0.264	0.225	0.393	0.395	0.393	0.629	0.091
0.376	0.388	0.497	0.307	0.275	0.440	0.476	0.516	0.706	0.098
0.298	0.269	0.356	0.315	0.258	0.410	0.471	0.456	0.627	0.105
0.308	0.316	0.444	0.300	0.299	0.475	0.439	0.484	0.690	0.112
0.379	0.395	0.481	0.319	0.301	0.470	0.515	0.543	0.722	0.119

Table 4.4 Sample features after discretization

RMA_X	RMA_Y	RMA_Z	RAA_X	RAA_Y	RAA_Z	ARE_X	ARE_Y	ARE_Z	Wear
(0.2, 0.25]	(0.25, 0.3]	(0.3, 0.35]	(0.25, 0.3]	(0.2, 0.25]	(0.3, 0.35]	(0.35, 0.4]	(0.35, 0.4]	(0.55, 0.6]	(0.05, 0.1]
(0.25, 0.3]	(0.25, 0.3]	(0.45, 0.5]	(0.25, 0.3]	(0.2, 0.25]	(0.35, 0.4]	(0.35, 0.4]	(0.35, 0.4]	(0.6, 0.65]	(0.05, 0.1]
(0.35, 0.4]	(0.35, 0.4]	(0.45, 0.5]	(0.3, 0.35]	(0.25, 0.3]	(0.4, 0.45]	(0.45, 0.5]	(0.5, 0.55]	(0.7, 0.75]	(0.05, 0.1]
(0.25, 0.3]	(0.25, 0.3]	(0.35, 0.4]	(0.3, 0.35]	(0.25, 0.3]	(0.4, 0.45]	(0.45, 0.5]	(0.45, 0.5]	(0.6, 0.65]	(0.1, 0.15]
(0.3, 0.35]	(0.3, 0.35]	(0.4, 0.45]	(0.25, 0.3]	(0.25, 0.3]	(0.45, 0.5]	(0.4, 0.45]	(0.45, 0.5]	(0.65, 0.7]	(0.1, 0.15]
(0.35, 0.4]	(0.35, 0.4]	(0.45, 0.5]	(0.3, 0.35]	(0.3, 0.35]	(0.45, 0.5]	(0.5, 0.55]	(0.5, 0.55]	(0.7, 0.75]	(0.1, 0.15]

After the feature selection process, two possible feature combinations were selected:

$$Reduct1 = \{RMA\_Y, RMA\_Z, RAA\_Z, ARE\_X, ARE\_Y, ARE\_Z\}$$

$$Reduct2 = \{RMA\_Y, RAA\_X, ARE\_X, ARE\_Y, ARE\_Z\}$$

Figure 4.1shows the tool wear estimation results using all the nine features presented in Table 4.2. Figure 4.2 and Figure 4.3 display the tool wear estimation results using two selected feature combinations.
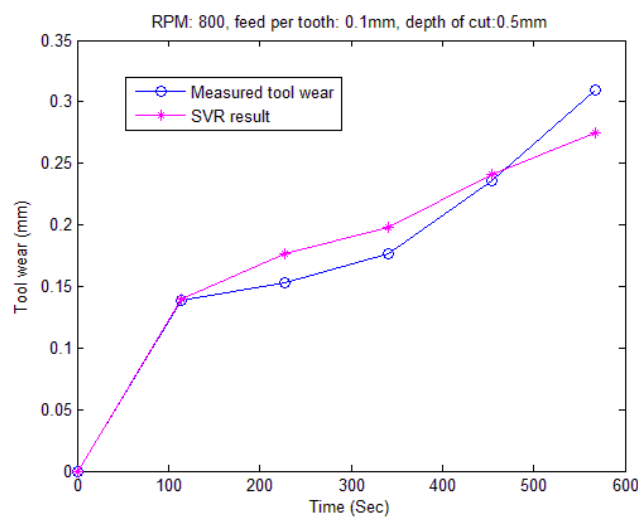
Figure 4.1 Measured and predicted tool wear based on all the candidate features (AAEE=0.0173)
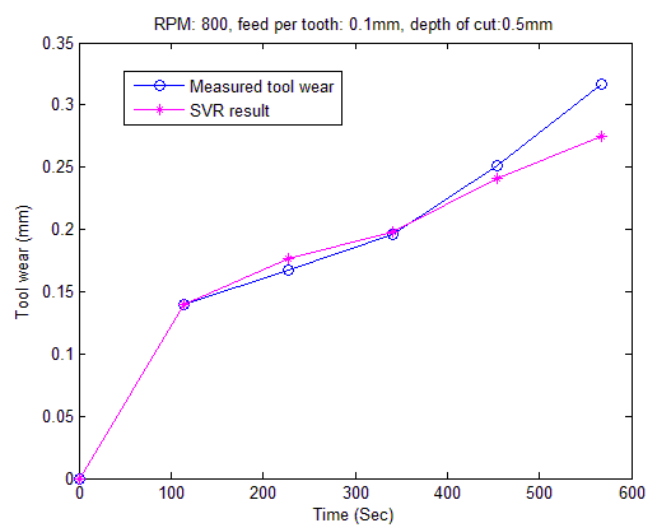
Figure 4.2 Measured and predicted tool wear based on selected feature set Reduct1 (AAEE=0.0126)
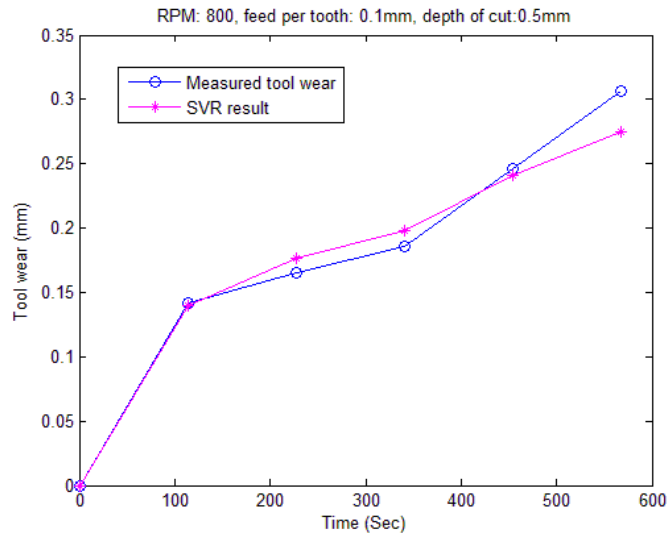
**Figure 4.3 Measured and predicted tool wear based
on selected feature set Reduct2 (AAEE=0.0127)**

Averaged Absolute Estimation Error (AAEE) is used to compare the accuracy:

$$\frac{\sum_{i=1}^{N} \left| VBm_i - VBe_i \right|}{N}$$

(4.7)

where *VBm* and *VBe* are measured and estimated tool wear.

A comparison of the results shows that the accuracy of tool wear estimation based on reduced feature combination was higher than that based on all the candidate features. The reduced feature combinations suggest that the energy features from the three axes cannot be eliminated. Apparently, the energy features are sensitive features for tool wear estimation. On the other hand, the maximum coefficient feature from the X axis was omitted in feature selection process. This result may be explained by the effect of cutting process direction on the signal strength. This may suggest that cutting direction should be taken into consideration when extracting features from cutting force data.

4.6 Conclusion

As the tool wear process is complex, there exist complementary, redundant and possibly conflicting interactions between some features in mapping their relation to the tool wear. Hence a proper feature selection process to identify an effective subset can improve efficiency and performance. In this investigation, the granularity structure of the cutting force features is studied using RST to find the optimal subset of features from the original set according to a given criterion.

Chapter 5

Model-based Tool Wear Profile Monitoring

5.1 Introduction

Average flank wear and maximum flank wear are commonly used as monitoring criteria in tool wear monitoring researches. In ball nose end milling applications, as the engagement changes continuously, present cutter-workpiece contact area may not be at the maximum tool wear location. Therefore, there is a need to monitor the tool wear profile along the cutting edge.

Subrahmanyam (2009) has developed a tool wear estimation model based on the geometrical model. However, the model depends upon the accumulated chip load and friction length information. In other words, the history of milling information must be recorded to predict future tool wear. This is suitable for new tool and is valuable in tool path planning to maximize the tool utilization and hence minimize the downtime. If a worn tool is used for machining, its history may not available and without the historical data, it is not possible to use the geometric tool wear model. In order to overcome this problem, this study focuses on monitoring the change of tool wear profile by monitoring the change of the cutting force based on the mechanistic cutting force model.

According to the mechanistic model, the cutting force can be split into a cutting force component and a ploughing force component. The cutting force component is the force required to remove the chip. The ploughing force is the force acting on the tool

edge and tool flank face (tool-workpiece interface region). The ploughing force increases when flank wear increases due to the friction at flank wear area. Therefore, it is possible to monitor the change of the area of flank wear by using the residual cutting force. Therefore, the aim of this study is to be able to determine the tool wear profile along the cutting edge for tool wear monitoring using the cutting force.

5.2 Problem formulation

In sculptured surface machining process, in addition to operating conditions (cutting speed, feed rate and depth of cut) relating to ball-nose end milling, the cutting engagement condition changes continuously (Ng et al., 2000).

Due to the geometrical nature of the ball-nose end mill, the angle between workpiece surface and the tool axis is less than $90°$. In normal practice, workpiece surface tilt angle can be varied according to the sculptured surface geometry. The effect of the surface angle on the tool wear estimation need to be considered. Therefore, when considering tool wear characteristics for tool condition monitoring, different tool orientation and workpiece angle need to be considered.

In this study, milling a hemispherical surface is designed for analyzing the cutting force signals in sculpture surface machining applications. In this experimental setup, there are two different tool orientations that can be tested in the experiments: horizontal downward; horizontal upward. In the designed milling process, the workpiece angle changes at different tool pass. Figure 5.1 shows an example of the change of workpiece angle when cutter orientation is horizontal downward. It also shows the different cutting condition at different path on the hemispherical surface.

Cutting force signals and tool wear measurement were obtained from the experiments under various machining conditions.

5.3 Experiments for milling of hemispherical surface

5.3.1 Workpiece material, cutting tool and equipment

Figure 5.1 shows the experimental setup for milling of hemispherical surface. The experiments were conducted on a 3-axis milling machine. The workpiece material was stainless steel. 10mm insert based coated carbide single flute ball nose end mills with 30 °helix angle were used in the experiments.

As this research focused on the correlation between tool wear and cutting force, one-flute cutter is preferred to ensure the measurements of cutting force and the tool wear are from same cutting edge. At the same time, the effect of run-out can be eliminated.

The cutting force was measured by a Kistler 9255B quartz 3-component platform dynamometer. The dynamometer was mounted between the workpiece and machining table. The cutting forces in the X, Y and Z directions were sampled by PC208AX Sony data recorder. The tool wear was measured using a Keyence microscope. A fixture was designed to measure the tool wear profile along the cutting edge.

5.3.2 Experimental parameters and procedure

The milling process in the experiments is at the finish stage to mill a workpiece with hemispherical surface. Different machining experiments were conducted from top to bottom or from bottom to up. Table 5.1 shows the cutting conditions.

The tool moves forward to create one horizontal cut on the hemispherical surface. The horizontal cuts were repeated at fixed pitch and depth of cut. For each path, the experiments were performed at different feed rate and spindle speed. The pitch feed of each path was 0.35 mm. Depth of cut was 0.3mm. Feedrate range was 0.05 mm/tooth/rev to 0.2 mm/tooth/rev. The cutting forces in the X, Y and Z directions were sampled with 3,000Hz sampling rate.

Table 5.1 Cutting conditions

Cutting Path Direction
Top to bottom
Bottom to top
Top to bottom followed by top to bottom
Top to bottom followed by bottom to top
Bottom to top followed by top to bottom
Bottom to top followed by bottom to top
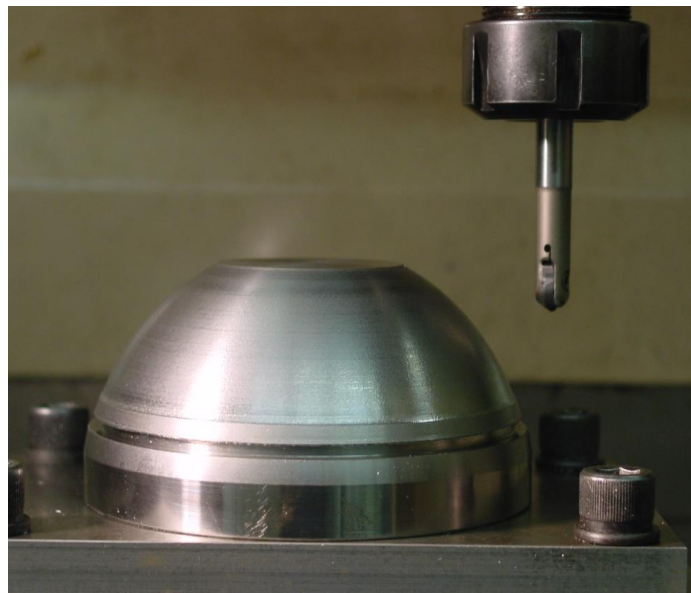
Figure 5.1 Milling hemispherical surface

5.4 Application of model-based tool wear monitoring framework

As typical ball nose end milling applications are sculptured surface machining, model-based tool wear monitoring framework discussed in Chapter 3 is validated at machining a hemispherical surface workpiece. Machining a hemispherical surface workpiece enables different contact points to be controlled and made between the ball-nose cutter and the workpiece. In the experiments, cutter path direction changes while the cutter is moving around the workpiece. This is particularly useful for capturing the necessary experimental data. In model-based tool wear monitoring framework, a cutting force model is adopted to simulate the cutting force when the tool moves along a tool path on sculptured surface. This provides the reference cutting force when the tool is in normal condition. The milling process is simulated by the use of geometrical model and cutting parameters along the tool path, such as the feed rate, depth of cut and cutting speed. The framework employs the discrete wavelet decomposition techniques to extract the maximum time-frequency information from the measured and simulated cutting forces. Features are extracted from the wavelet coefficients of the measured cutting force and simulated cutting force. Suitable features are those that are sensitive to tool wear when ball-nose end milling sculptured surface. Relevant features are selected using discernibility-based data analysis based on rough set theory (RST). Support vector machine for regression (SVR) is proposed to map the features (input) to tool wear level (output) by training via examples.

The implementation procedures are presented as follows:

(1) **Cutting force model building.** The tool pass on the workpiece is shown in Figure 5.2. As shown in Figure 5.2, one tool pass is the complete circular

travel around the workpiece. After one tool pass is completed, the tool starts at next pass at fixed pitch feed until the end of the surface. The model proposed for inclined plane machining is used to estimate the cutting force by assuming the workpiece as straight inclined plane at the tool workpiece contact point (Subrahmanyam, 2009). The cutting force is estimated at tool contact point using given cutting conditions such as feed rate, depth of cut, cutter path direction and workpiece inclination angle.

Workpiece
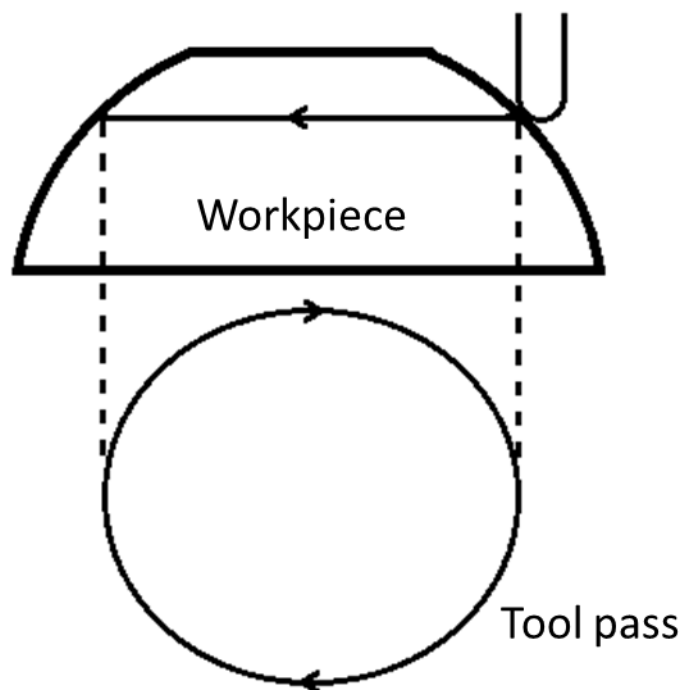
Tool pass

Figure 5.2 Tool pass on the workpiece

a. Mechanistic cutting force model. The differential cutting forces in tangential, radial and axial direction, and can be expressed as a function of cutter rotation angle and axial position:

$$\begin{cases} dF_t = K_{te} \cdot dS(z) + K_{tc} \cdot t(\varphi) \cdot db \\ dF_r = K_{re} \cdot dS(z) + K_{rc} \cdot t(\varphi) \cdot db \\ dF_a = K_{ae} \cdot dS(z) + K_{ac} \cdot t(\varphi) \cdot db \end{cases} \tag{5.1}$$

where F_t, F_r, F_a are elemental tangential, radial, and axial cutting forces, (K_{te}, K_{re}, K_{ae}) are edge force coefficients, (K_{tc}, K_{rc}, K_{ac}) are shearing coefficients, dS is the differential length of the curved cutting edge segment, $t(\phi)$ is the undeformed chip thickness normal to the cutting edge, db is the chip width in each cutting edge discrete element.

b. Determine ball-nose end milling cutting force model coefficients. For a particular workpiece-cutter combination, the average force data measured in a set of model building experiments are required to identify the numerical values of the model parameters. The average cutting force per tooth period is independent of the helix angle. The integration for the average force of the measured force is done in one revolution. In order to get the calculated force, the cutting force is integrated axially at each incremental rotation angle, from the bottom disc to the upper disc at axial depth of cut. By comparing the calculated equation with the experimental average cutting force values, the cutting force model coefficients can be identified.

c. From the experiments, the measured cutting force follows the X, Y and Z-directions of dynamometer. However, while machining on the hemispherical surface workpiece, the cutter is moving around the workpiece. Hence the simulated cutting force is calculated at the tool moving direction around the workpiece. The measured cutting forces

are transformed to the same direction of simulated cutting force at the tool workpiece contact point. In this way, the simulated cutting force can be compared with the measured cutting force.

(2) **Signal processing using Wavelet**. In order to maximize the information utilization of cutting force signals, features are extracted from the wavelet coefficients. Since Daubechies wavelets perform well in separating the frequency bands during signal decomposition, they are selected for feature extraction in this research. In this test, the wavelet transformation of cutting force was repeated twice to obtain the coefficients in subsequent experiments. Through wavelet transformation, the experimental cutting force data were decomposed into the constituent parts at frequency bands [1 Hz, 375 Hz], [376 Hz, 750 Hz] and [751 Hz, 1500 Hz], respectively.

(3) **Feature extraction.** Due to the fact that the energy of cutting force tends to be concentrated at tooth passing frequency and its low frequency harmonics, the energy level of the low frequency band is much higher than that of middle and high frequency band. Cutting force data in low frequency band can be extracted for feature extraction. After the cutting force is decomposed through wavelet transform, the low frequency band of signal is represented by the approximation coefficients. Therefore, the wavelet approximations of the force data are used for feature extraction. Tool wear states are reflected by the varied characteristics of the extracted features. To obtain feature vectors from the cutting force model, the measured and simulated cutting force are processed through wavelet transform. The residual difference between the measured and simulated approximation coefficients can be a sensitive feature vector, which is used for the evaluation of the difference between measured

force and simulated force. When the tool is in good condition, this measure has the lower value which shows the force signals are well matched. Three kinds of residual measurements are used in this work:

    a. Residual Maximum Approximation Coefficients (RMA):

$$RMA = (\max(A_m) - \max(A_s)) / \max(A_s) \qquad (5.2)$$

    b. Residual Average Approximation Coefficients (RAA):

$$RAA = (\overline{A}_m - \overline{A}_s) / \overline{A}_s \qquad (5.3)$$

    c. Average Residual Energy (ARE):

$$ARE = \frac{1}{N} \sum_{i=1}^{N} ((A_m(i))^2 - (A_s(i))^2) \qquad (5.4)$$

where $A_m(i)$ and $A_s(i)$ are wavelet approximation coefficients from measured cutting force and simulated cutting force respectively, N is the total number of wavelet coefficients.

(4) **Feature selection.** Relevant features are selected using discernibility-based data analysis based on rough set theory (RST). According to the feature selection results discussed in Chapter 4, the most effective feature set includes following features:

    a. Residual Maximum Approximation Coefficients at Y direction (RMA_Y)

    b. Residual Maximum Approximation Coefficients at Z direction (RMA_Z)

    c. Residual Average Approximation Coefficients at Z direction (RAA_Z)

    d. Average Residual Energy at X direction (ARE_X)

e.   Average Residual Energy at Y direction (ARE_Y)

f.   Average Residual Energy at Z direction (ARE_Z)

This feature set is used as input of support vector machines to estimate the tool wear.

(5) **Decision making using support vector machine for regression (SVR).** The application of SVR has been discussed in Chapter 3. In this test, Gaussian kernel is chosen as the kernel function:

$$K(\mathbf{x}_i, \mathbf{x}_j) = \exp\left(-\frac{\left\| \mathbf{x}_i - \mathbf{x}_j \right\|^2}{2\sigma^2} \right) \tag{5.5}$$

To construct the SVR model, the training data sets are obtained under various cutting parameters used in the experiment. There are total six datasets with different cutting conditions. Two datasets are used as training dataset, while the other four datasets are used as test dataset.

When the tool mills the surface at a specific cutting pass, the tool wear area in current cutter-workpiece contact area is selected as a measure of tool wear level. After tool wear is generated by the milling at a specific cutting pass, the milling at the next pass will generate tool wear over the previous tool wear in the overlapped portion. The residual cutting force feature is correlated with the tool wear area in the tool-workpiece contact area at current pass. In order to extract training data from the test dataset, the current tool wear area in the tool-workpiece contact area is determined by interpolation method.

5.5 Experimental results and discussion

5.5.1 Interpolation of tool wear for training data

When the tool mills the surface at a specific cutting pass, the tool wear area in current cutter-workpiece contact area is selected as a measure of tool wear level. After tool wear is generated by the milling at a specific cutting pass, the milling at the next pass will generate tool wear over the previous tool wear in the overlapped portion. The residual cutting force feature is correlated with the tool wear area in the tool-workpiece contact area at current pass. In order to extract training data from the test dataset, the current tool wear area in the tool-workpiece contact area needs to be determined.

The tool wear was measured after the whole hemispheric surface was milled. As all of the cutting passes overlapped, the measurement of tool wear at certain angular location at the cutting edge would have been the cumulated effect of tool wear due to all of the cutting passes at the particular angular location. The measured tool wear is therefore not the tool wear profile when milling a specific pass. This means that the measured tool wear has to be decomposed tool wear profiles from each pass.

The tool wear profile at the tool-workpiece contact area when milling a specific pass can be simulated by the geometric tool wear model. The value of tool wear area is used to train the SVR to build the tool wear estimation model. After training, the tool wear estimation model can be used to predict the tool wear area in the range of engaged cutting edge at specific pass.

Subrahmanyam (2009) has developed a tool wear estimation model based on the geometrical model. In general, the flank wear is developed in three stages: rapid initial stage, progressive wear stage, and rapid wear stage. This study investigates the change of tool wear profile in progressive wear stage as most of tool useful life is in this stage. In this stage, the tool wear increases steadily according to the chip load and friction length. Therefore, geometric tool wear model can be used to simulate tool wear profile at each pass.
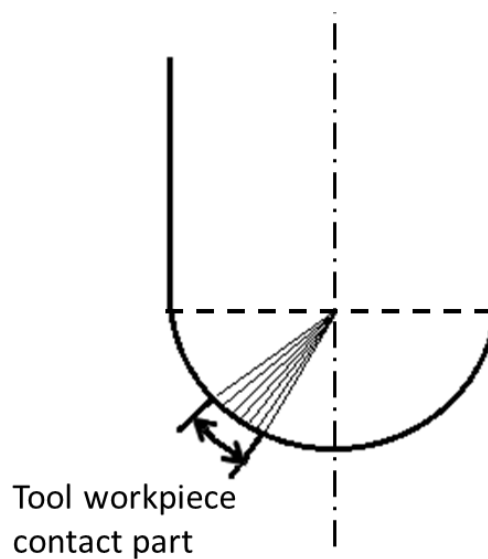
Figure 5.3 Cutting edge elements for ball nose end mill

Figure 5.3 shows the cutting edge which is equally divided into a finite number of cutting edge elements represented in degrees. When milling one pass, the portion of the cutting edge that contacts with the workpiece comprises a certain number of the cutting edge elements. One element may contact with the workpiece at different pass due to the overlap of the contact area for the neighboring passes. By using the geometric tool wear model, the tool wear at each element can be simulated by the chip load and friction length. The tool wear value of all the cutting edge elements in current tool-workpiece contact area represents the tool wear profile at current pass.

Subrahmanyam (2009) has developed the equation for the model as follows:

$$tw_i = k_3 \times \left[\int cl_i dt \right]^{\alpha} \times \left[\int fl_i dt \right]^{\beta} \times \left[ttw_i \right]^{\gamma} \qquad (5.6)$$

where $ttw_i = \left(\dfrac{1}{1 - k \times tw_{i(t-1)}} \right)$

'tw_i' is tool wear for 'i^{th}' number of cutting edge, '$tw_{i(t-1)}$' is tool wear for 'i^{th}' cutting edge estimated in earlier pass. 'cl_i' and 'fl_i' are the total chip load removed by 'i^{th}' cutting edge. The integrated value represents the accumulated chip load and friction length for entire tool path, and 'k_3', 'α', 'β' 'γ' and 'k' are model parameters.

The tool wear at current cutting edge element is estimated by three components: the chip load, the friction length and the tool wear feedback of previous pass. The change of engagement of each pass can be represented by the change of group of cutting edge elements. The change of cutting conditions for each pass, such as depth of cut, feed rate, inclination angle and cutter path direction, will be modeled as chip load and friction length at the geometric tool wear estimation model.

Figure 5.4 shows tool wear profile simulation using geometric tool wear estimation model at specific cutting pass. As the cutting force measurement is pass-by-pass, the tool wear profile at each cutting pass need to be simulated so that the cutting force can be monitored pass-by-pass to estimate the value of tool wear area.
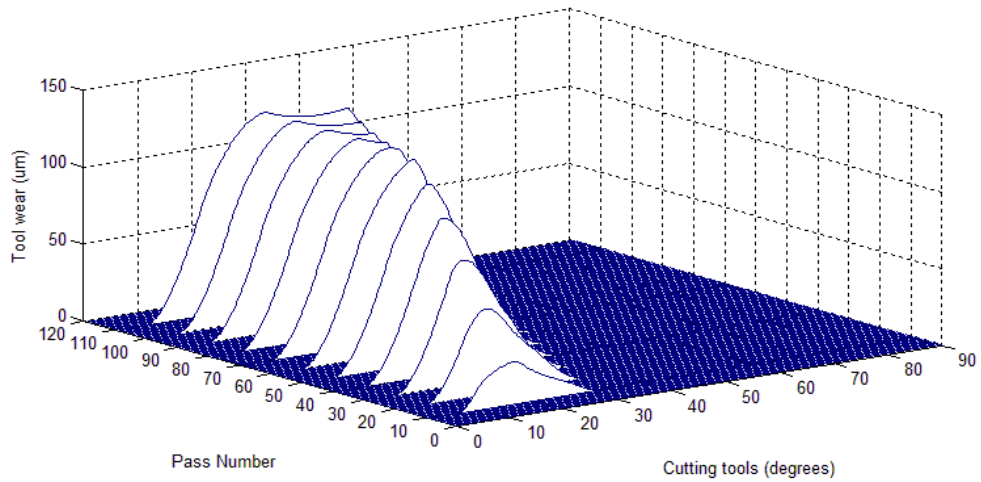
Figure 5.4 Tool wear profile simulation at specific cutting pass
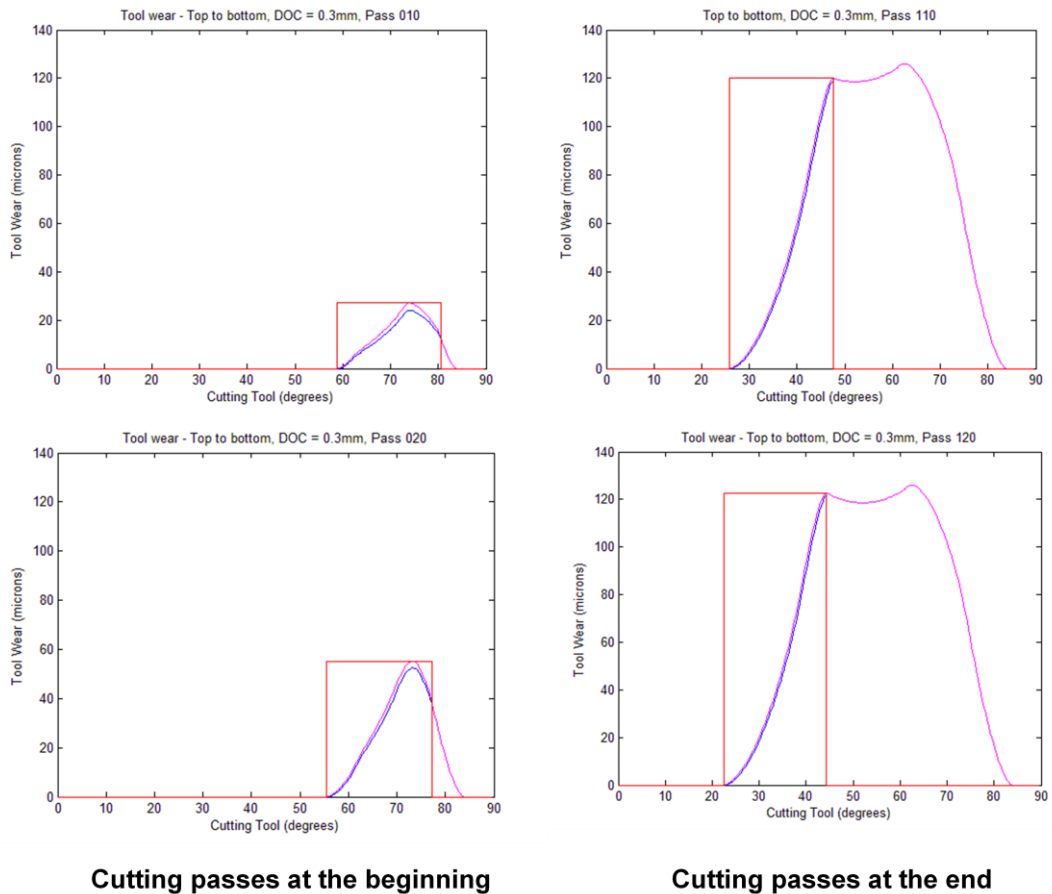
Figure 5.5 Tool wear areas when milling hemispherical surface using a new tool
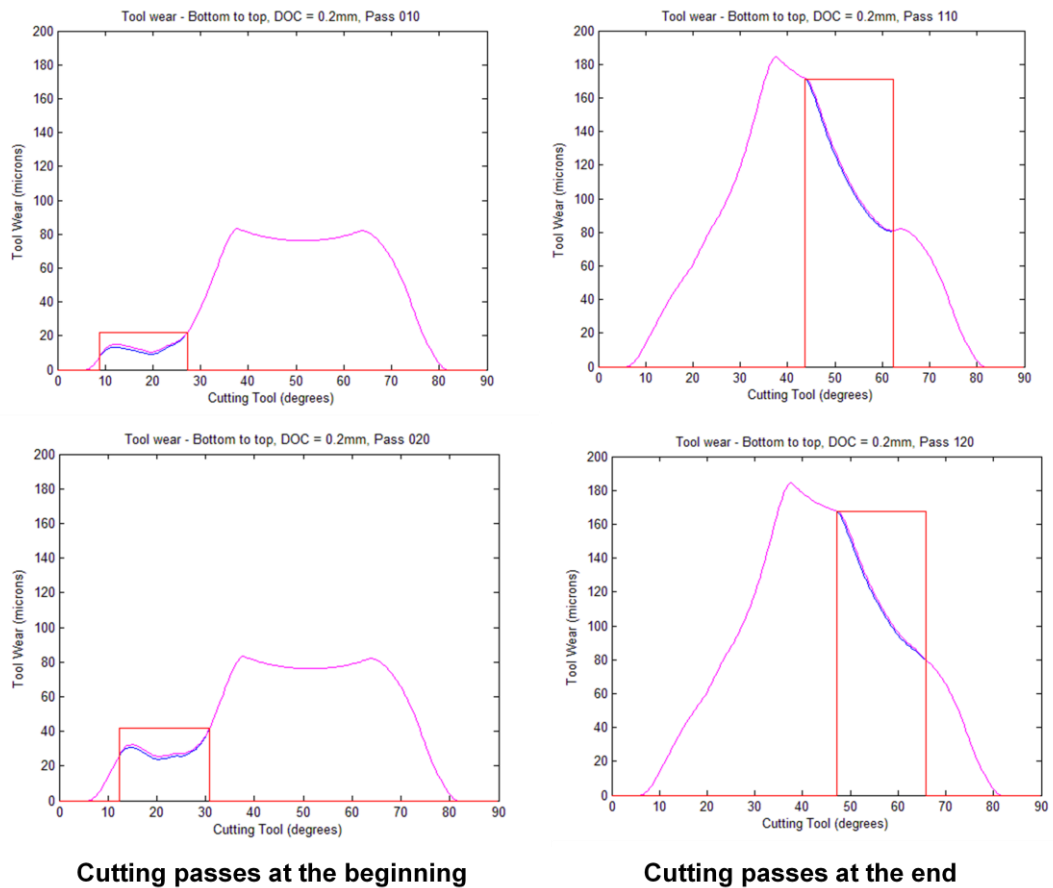
Figure 5.6 Tool wear areas when milling hemispherical surface using a worn tool

5.5.2 Tool wear estimation

Figure 5.5 and Figure 5.6 show the tool wear area at the end of specific cutting passes. In the figures, the rectangle shows the angle range of tool-workpiece contact area. The value of tool wear area in the cutter-workpiece contact area can be predicted using residual cutting force features. Figure 5.7 shows the tool wear area prediction result when milling hemispherical surface from top to bottom using a new tool. Figure 5.8 shows the tool wear area prediction result when milling hemispherical surface from bottom to top when using a worn tool. The worn tool has been used to mill the hemispherical surface from top to bottom.
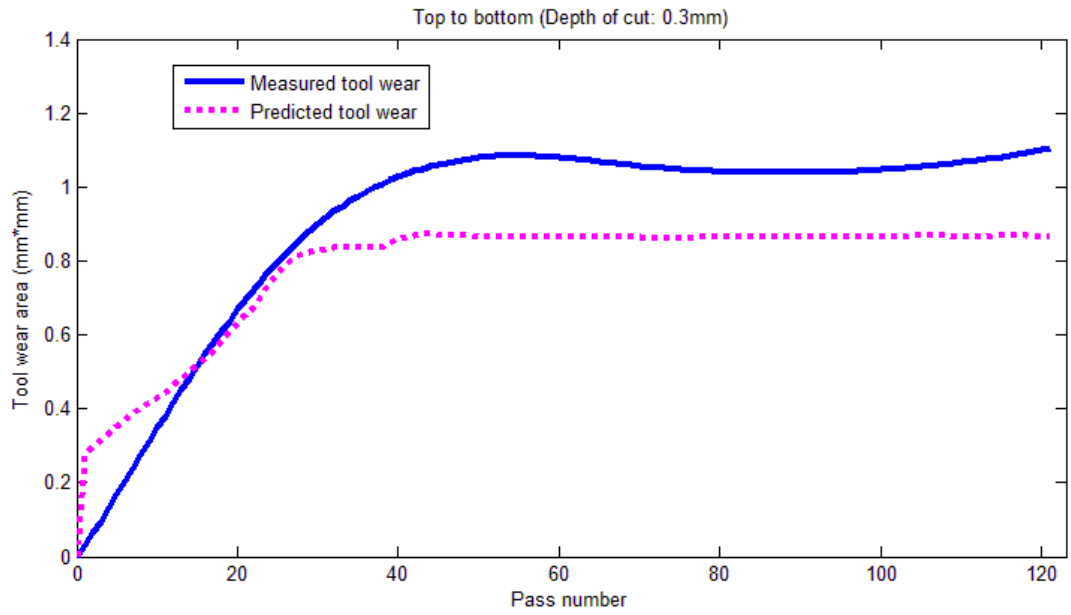
Figure 5.7 Tool wear estimation when milling hemispherical surface using a new tool
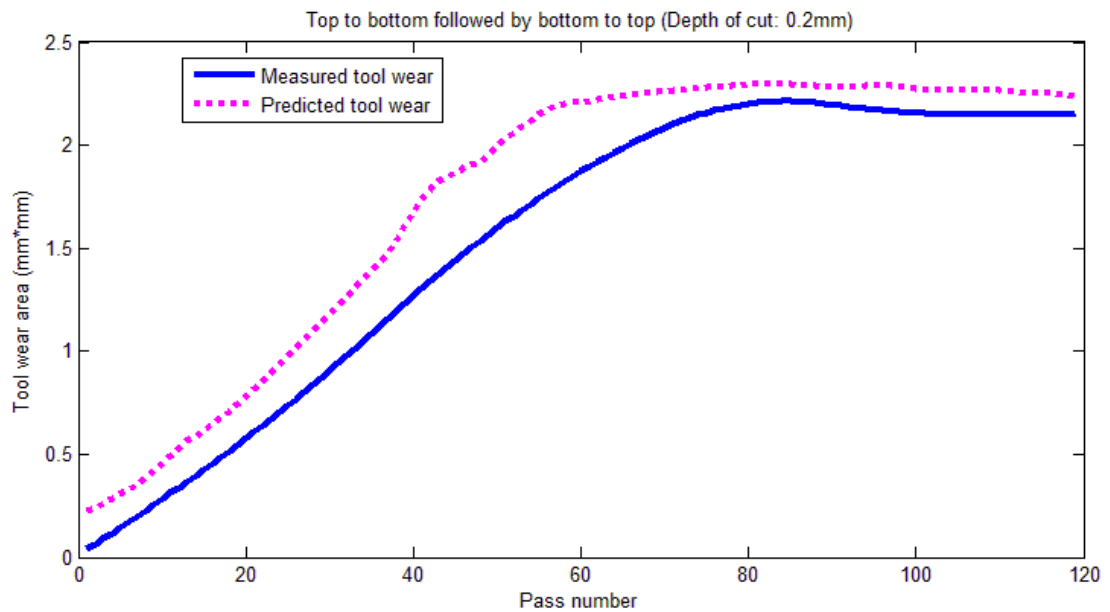
Figure 5.8 Tool wear estimation when milling hemispherical surface using a worn tool

Comparing Figure 5.5 and Figure 5.6, the tool wear distribution in the cutter-workpiece contact area is quite different. It may affect the accuracy of the results of tool wear profile prediction. When the tool wear distribution is not uniform in current cutter-workpiece contact area, the tool wear prediction may be less accurate.

5.6 Conclusion

This study is to monitor tool wear profile along the cutting edge using cutting force. The residual cutting force feature is correlated with the tool wear area in current engaged cutting edge. Firstly, this method has considered the accumulated tool wear from different cutter-workpiece contact area. Secondly, the effective chip load at different section in the same contact area is different for each specific tool pass. The geometric modeling method was used to evaluate the chip load of the contact section of the cutting edge with workpiece. Thirdly, overlapped cutting passes are considered in this method. Fourthly, two different tool orientations have been tested in the experiments: horizontal downward; horizontal upward.

Chapter 6

Conclusions and Recommendations

6.1 Conclusions

Using sensors to estimate tool wear is a very important function to improve workpiece quality and accuracy in ball-nose end milling process. Among various sensors, cutting force sensor is the most suitable sensor in end milling process. This research proposed a model-based tool wear estimation framework using cutting force to monitor ball-nose end milling process. This framework should help contribute to the reduction of production cost and the improvement of product quality in mould and die industry. The proposed framework comprised three parts: feature extraction from cutting force data; feature selection; tool wear estimation using support vector machines for regression (SVR). The following are the contributions reported in this thesis:

1. One key contribution in this study is the development of a model-based method to extract the features from cutting force data and use the features extracted as inputs of the SVR for tool wear estimation. Feature extractions were conducted based on the discrete wavelet transform (DWT) techniques. Cutting force data were collected and processed using wavelet technique. To determine the useful frequency band of the decomposed data for feature extraction, energy distribution using DWT was evaluated. Support vector machines for regression (SVR) were trained by the feature vectors to build a tool wear estimation model to on-line predict tool wear. The experimental results show that the model-based approach is feasible and effective.

2.	This study has identified and developed energy related features as effective features for input to the SVR. Another contribution of the study is in the development of a method for the selection of relevant and effective features to improve the efficiency and accuracy of the aforementioned approach. An integrated feature selection methodology based on rough set theory (RST) and support vector machine for regression (SVR) has been proposed in this study. The results showed that it is possible to use RST to reduce feature space and improve the accuracy of tool wear estimation. In this method RST is applied for the first time in feature selection in tool wear estimation. Presently, different approaches have been used to find reducts in RST. In future study, the optimal reducts seeking approach can be explored.

3.	Based on the extracted features from cutting force data, a machine learning method has been investigated to build an efficient regression model for tool wear estimation. The machine learning method used in this work is support vector machines for regression (SVR). In this study, kernel selection methodologies were explored to find optimal kernel, including the type of kernel and kernel parameters. Experimental results showed that the proposed method can effectively estimate the tool wear to improve the machining quality. Compared with artificial neural networks (ANN) method, SVR overcomes the over-parameterization and non-convergence problems. When the size of training data set was small, the accuracy of tool wear estimation using SVR was better than ANN method. The reason could be that the SVR takes advantage of prior knowledge of tool wear and construct a hyper-plane as the decision surface. Experimental results also showed that the SVR performances were quite different when four kinds of kernel were used for tool wear estimation applications. It can be observed from the results that kernel selection is one of the main reasons that affect the tool wear estimation performance.

4. Reliability is the main concern for preventing widespread adoption of tool condition monitoring techniques. Most of present monitoring systems only determine the presence of the fault, that means the decision is either tool worn or tool not worn (binary identification) (Teti et al., 2010). In industrial environment, many unpredicted factors, such as stochastic influence from workpiece composition, vibration, and machine noise, may cause interference to the results of tool condition monitoring. Hence the false prediction is unavoidable. It is very difficult to identify the false prediction for tool condition monitoring system with binary identification. In order to improve the reliability of tool condition monitoring system, multi-classification of tool state or tool wear estimation methods are explored to avoid the unnecessary tool replacement or workpiece damage. In common industrial practice, tool wear does not mean the end of useful tool life in most cases. If the tool wear is tolerable, the machinist may decide to continue using the tool in subsequent tool path. Tool wear monitoring methods can help machinists to monitor the tool wear process from initial wear state to severe wear state. In this way, instead of providing binary identification of tool state (tool worn or tool not worn), the threshold-based tool wear monitoring system monitors the tool wear in real-time. The machinist can be alerted if the machining process needs to be supervised closely when tool wear is over certain limit. In summary, tool wear monitoring methods have been developed to overcome the limitation of binary identification and to improve reliability.

5. Another important concern for industrial application is the deployability of TCM system. As large number of test cuts is required to build a TCM system, the requirement on test cuts makes TCM system only suitable for large scale production. Ball-nose end milling is normally one-off or small batch milling application. Trial machining of some workpieces is time-consuming and very expensive for one-off or

small batch milling applications. As the data of test cuts are difficult to obtain, the TCM system is not easy to be adopted in the industrial applications. To avoid the large amounts of empirical data collection, cutting force model based tool condition monitoring has been explored in this study.

6.2 Recommendations for future work

6.2.1 Inexpensive alternative sensors

The cost is one of the factors affecting the application of tool condition monitoring system (TCM) in industry. In order for industry to adopt sensor based TCM system cost-effective solutions should be provided.

Cutting force is usually considered as one of the most reliable measurement to monitor the tool condition (Cui, 2008). However, cutting force sensors are very expensive. If the cost-performance ratio of TCM system is very high due to the expensive sensors, industry may not accept the well-known TCM method to prevent damage and improve quality in machining. Therefore, inexpensive alternative sensors are explored for TCM system.

Li et al. (Li et al., 2004) developed a hybrid mathematical-fuzzy method to estimate the feed-cutting force using inexpensive current sensors. The estimated cutting force is employed to monitor the tool wear in a computerized numerical control (CNC) turning center. But the proposed method is not suitable for milling process with intermittent nature. It is an interesting research topic to make use of inexpensive current sensors to monitor tool condition in milling.

Recently, an energy based cutting force model was proposed to estimate cutting force using an inexpensive and non-invasive spindle motor power sensor in end milling (Xu et al., 2007). One research topic is to explore the reliable correlations between the coefficients of cutting force model and tool conditions including the type and extent of tool damage (Jerard et al., 2008). Another research topic is to overcome the limited bandwidth from the data sources of power sensor.

6.2.2 Base wavelet selection

Wavelet selection is an important factor in improving the performance of the SVR model. In wavelet analysis any wavelet can be selected as the basis function, but the quality of the results depends on the selected wavelet. A suitable wavelet needs to be selected to produce the best results for feature extraction in the cutting force signals.

The family of Daubechies wavelets is chosen as the basis functions in most of the fault diagnostics applications. Daubechies wavelets are classified according to the number of vanishing moments. To investigate the influence of the number of vanishing moments, typical wavelets, db4, db8 and db20 have been used to process cutting force data for feature extraction. The same testing set was used for the comparison of the performance of tool wear estimation by different wavelets. Figure 6.1 shows that the SVR results are quite different for different wavelets. In these results, averaged absolute estimation errors (AAEE) of db2, db4 and db10 are 8.9 μm, 10.0 μm and 13.6 μm respectively. From the result, it is clear that the AAEE for Gaussian kernel with db2 wavelet is 8.9 μm. This AAEE value is the smallest compared with those for the other wavelets. Therefore, it will be an interesting research topic to choose the most efficient wavelet for tool condition monitoring. Base wavelet selection criteria need to be developed to evaluate different wavelets.
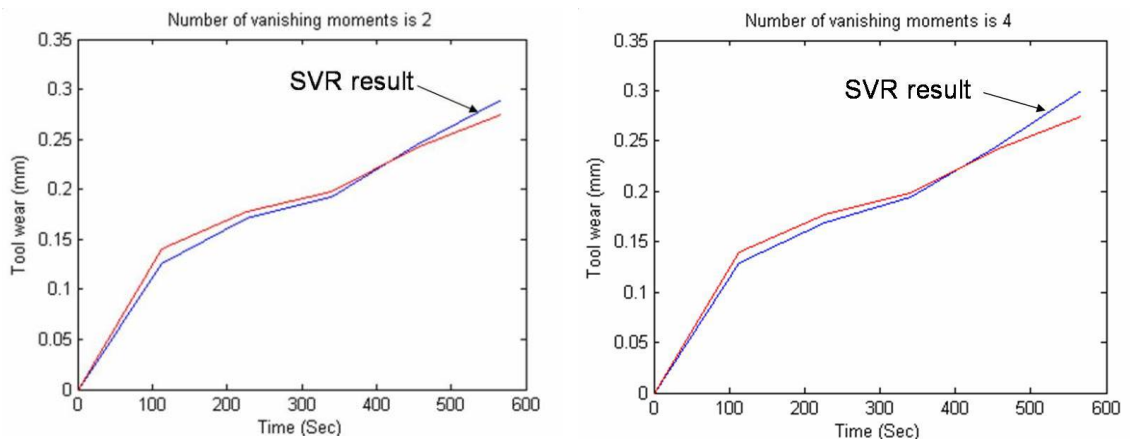
(1) Number of vanishing moment is 2   (2) Number of vanishing moment is 4
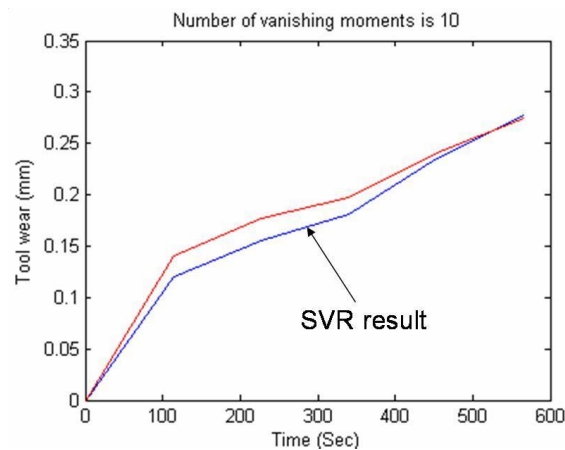
(3) Number of vanishing moment is 10

Figure 6.1　Comparison of SVR results using different wavelet for signal processing

6.2.3　Extract features using pattern recognition methods

To determine the tool wear by measured cutting force, the feature will be extracted from the measured cutting force and the simulated force with different flank wear. The similarity between the feature vectors from measured cutting force and simulated cutting force is a kind of sensitive features. When the tool is in good condition, these measures have the lower values which show the force signals are well matched.

Let $C_m(i)$ and $C_s(i)$ be the wavelet coefficients from measured cutting force and simulated cutting force respectively, N be the total number of wavelet coefficients, following similarity measures are possible features:

Relative Residual (RR):

$$RR = \sqrt{\frac{\sum_{i=1}^{N} (C_m(i) - C_s(i))^2}{\sum_{i=1}^{N} (C_s(i))^2}} \tag{6.1}$$

Wavelet Distance (DIST):

$$DIST = \sum_{j=1}^{M} \sum_{i=1}^{N_j} \frac{|C_m(i,j) - C_s(i,j)|}{|C_s(i,j)|} \tag{6.2}$$

Correlation Coefficient (CC):

$$CC = \frac{\sum_{i=1}^{N} (C_m(i) - \overline{C}_m)(C_s(i) - \overline{C}_s)}{\sqrt{\sum_{i=1}^{N} (C_m(i) - \overline{C}_m)^2 \sum_{i=1}^{N} (C_s(i) - \overline{C}_s)^2}} \tag{6.3}$$

Residual Difference(RD):

$$RD = \frac{\sum_{i=1}^{N} (C_m(i) - C_s(i))^2}{\sqrt{\sum_{i=1}^{N} (C_m(i) - \overline{C}_m)^2 \sum_{i=1}^{N} (C_s(i) - \overline{C}_s)^2}} \tag{6.4}$$

6.2.4 Kernel selection

The kernel function is used for nonlinear mapping the input features into a higher dimensional feature space, and thus linear regression in the feature space is feasible. The optimal kernel (including the type of kernel and kernel parameters) is needed to get the high generalization performance to estimate tool wear. The polynomial kernel,

Gaussian kernel, Sigmoid kernel and spline kernel are the commonly used kernels for support vector machines.

The polynomial kernel function is

$$K(\mathbf{x}, \mathbf{x}_i) = \left(\mathbf{x}^T \mathbf{x}_i + 1\right)^p \tag{6.5}$$

The Gaussian kernel function is

$$K(\mathbf{x}, \mathbf{x}_i) = \exp\left(-\frac{\|\mathbf{x} - \mathbf{x}_i\|^2}{2\sigma^2}\right) \tag{6.6}$$

The Sigmoid kernel function is

$$K(\mathbf{x}, \mathbf{x}_i) = \tanh\left(\beta_0 \mathbf{x}^T \mathbf{x}_i + \beta_1\right) \tag{6.7}$$

The spline kernel is

$$K(\mathbf{x}, \mathbf{x}_i) = 1 + \left(\mathbf{x}^T \mathbf{x}_i\right) + \frac{1}{2}\left(\mathbf{x}^T \mathbf{x}_i\right)\min\left(\mathbf{x}^T \mathbf{x}_i\right) - \frac{1}{6}\min\left(\mathbf{x}^T \mathbf{x}_i\right)^3 \tag{6.8}$$

A preliminary study was conducted by using 4 different kernels to estimate the tool wear for the same data set and same feature extraction methods. The performances are quite different when four kinds of kernel are used for tool wear estimation applications. To compare the performance of the regression results from different kernel, averaged absolute estimation errors (AAEE) are shown in Table 6.1. It can be observed from the results that kernel selection will affect the tool wear estimation performance.

Table 6.1 Comparison of tool wear estimation using different kernel function

Kernel Function	AAEE
1. The polynomial kernel	6.3 μm
2. The Gaussian kernel	10.0 μm
3. The Sigmoid kernel	14.8 μm
4. The spline kernel	34.1 μm

One of the possible kernel selection methods is meta-learning for support vector machines (Ali and Smith-Miles, 2006). This method is to determine which kernel can get optimal performance for specific classification application. To improve this approach into regression applications, the performance evaluation function needs to be identified to evaluate the performance of SVR with difference kernel functions.

References

ALI, S. & SMITH-MILES, K. A. 2006. A meta-learning approach to automatic kernel selection for support vector machines. *Neurocomputing,* 70**,** 173-186.

ALTINTAS, Y. 2000. *Manufacturing Automation: Metal Cutting Mechanics, Machine Tool Vibrations, and CNC Design*, Cambridge University Press.

AMER, W., GROSVENOR, R. I. & PRICKETT, P. W. 2006. Sweeping filters and tooth rotation energy estimation (TREE) techniques for machine tool condition monitoring. *International Journal of Machine Tools & Manufacture,* 46**,** 1045-1052.

BALAZINSKI, M., CZOGALA, E., JEMIELNIAK, K. & LESKI, J. 2002. Tool condition monitoring using artificial intelligence methods. *Engineering Applications of Artificial Intelligence,* 15**,** 73-80.

BHATTACHARYYA, P. & SANADHYA, S. K. 2006. Support Vector Regression Based Tool Wear Assessment in Face Milling. *IEEE International Conference on Industrial Technology. ICIT 2006.*

BHATTACHARYYA, P., SENGUPTA, D. & MUKHOPADHYAY, S. 2007. Cutting force-based real-time estimation of tool wear in face milling using a combination of signal processing techniques. *Mechanical Systems and Signal Processing,* 21**,** 2665-2683.

BYRNE, G., DORNFELD, D., INASAKI, I., KETTELER, G., KONIG, W. & TETI, R. 1995. Tool condition monitoring (TCM) - the status of research and industrial application. *CIRP Annals - Manufacturing Technology,* 44**,** 541-567.

CHANG, T. C., WYSK, R. A. & WANG, H. P. 2006. *Computer-aided Manufacturing*, Pearson Education Inc.

CHEN, J. C. & CHEN, W. 1999. A tool breakage detection system using an accelerometer sensor. *Journal of Intelligent Manufacturing,* 10**,** 187-197.

CHEN, S. L. & JEN, Y. W. 2000. Data fusion neural network for tool condition monitoring in CNC milling machining. *International Journal of Machine Tools & Manufacture,* 40**,** 381-400.

CHO, S., ASFOUR, S., ONAR, A. & KAUNDINYA, N. 2005. Tool breakage detection using support vector machine learning in a milling process. *International Journal of Machine Tools and Manufacture,* 45**,** 241-249.

CHOI, B. K. 1991. *Surface Modeling for CAD/CAM*, Elsevier Science Publishers B.V.

CHOI, B. K. & JERARD, R. B. 1998. *Sculptured Surface Machining - Theory and Applications*, Kluwer Academic Publishers.

CHOI, Y., NARAYANASWAMI, R. & CHANDRA, A. 2004. Tool wear monitoring in ramp cuts in end milling using the wavelet transform. *The International Journal of Advanced Manufacturing Technology,* 23**,** 419-428.

CUI, Y. 2008. *Tool wear monitoring for milling by tracking cutting force model coefficients.* Master of Science, University of New Hampshire.

DIMLA, E. D., SNR. 2000. Sensor signals for tool-wear monitoring in metal cutting operations - a review of methods. *International Journal of Machine Tools & Manufacture,* 40**,** 1073-1098.

DIMLA JR, D. E., LISTER, P. M. & LEIGHTON, N. J. 1997. Neural network solutions to the tool condition monitoring problem in metal cutting—A critical review of methods. *International Journal of Machine Tools and Manufacture,* 37**,** 1219-1241.

DONG, J., SUBRAHMANYAM, K. V. R., WONG, Y. S., HONG, G. S. & MOHANTY, A. 2006. Bayesian-inference-based neural networks for tool wear estimation. *The International Journal of Advanced Manufacturing Technology,* 30**,** 797-807.

DORNFELD, D. 2003. Future directions in manufacturing research. *NSF Workshop.* Madison, WI.

DU, R. 1999. Signal understanding and tool condition monitoring. *Engineering Applications of Artificial Intelligence,* 12**,** 585-597.

DUAN, K., KEERTHI, S. S. & POO, A. N. 2003. Evaluation of simple performance measures for tuning SVM hyperparameters. *Neurocomputing,* 51**,** 41-59.

FENG, H. Y. & MENQ, C. H. 1994. The prediction of cutting forces in the ball-end milling process - I. Model formulation and model building procedure. *International Journal of Machine Tools & Manufacture,* 34**,** 697-710.

GAING, Z. L. 2004. Wavelet-Based Neural Network for Power Disturbance Recognition and Classification. *IEEE Transactions on Power Delivery,* 19**,** 1560-1568.

GHOSH, N., RAVI, Y. B., PATRA, A., MUKHOPADHYAY, S., PAUL, S., MOHANTY, A. R. & CHATTOPADHYAY, A. B. 2007. Estimation of tool wear during CNC milling using neural network-based sensor fusion. *Mechanical Systems and Signal Processing,* 21**,** 466-479.

HAYKIN, S. 1999. *Neural Networks: A Comprehensive Foundation,* Upper Saddle River, Prentice-Hall.

HONG, G. S., RAHMAN, M. & ZHOU, Q. 1996. Using Neural Network for Tool Condition Monitoring Based on Wavelet Decomposition. *International Journal of Machine Tools & Manufacture,* 36**,** 551-566.

HUANG, C. L., LI, T. S. & PENG, T. K. 2005. A hybrid approach of rough set theory and genetic algorithm for fault diagnosis. *The International Journal of Advanced Manufacturing Technology,* 27**,** 119-127.

HUANG, S., GOH, K. M., SHAW, K. C., WONG, Y. S. & HONG, G. S. 2007a. Model-based monitoring and failure detection methodology for ball-nose end milling. *IEEE Conference on Emerging Technologies and Factory Automation*

HUANG, S., ZHANG, D. H., LEONG, W. Y., CHAN, H. L., GOH, K. M., ZHANG, J. B. & KRISTO 2008. Detecting tool breakage using accelerometer in ball-nose end milling. *International Conference on Control, Automation, Robotics and Vision.*

HUANG, S. N., TAN, K. K., WONG, Y. S., DE SILVA, C. W., GOH, H. L. & TAN, W. W. 2007b. Tool wear detection and fault diagnosis based on cutting force monitoring. *International Journal of Machine Tools & Manufacture,* 47**,** 444-451.

ISO 1989. ISO 8688-2 Tool life testing in milling - Part 2: End milling. International Organization for Standardization.

JEMIELNIAK, K. 1999. Commercial tool condition monitoring systems. *The International Journal of Advanced Manufacturing Technology,* 15**,** 711-721.

JERARD, R. B., FUSSELL, B. K., DESFOSSES, B., XU, M., JAVOREK, B., CUI, Y., NICHOLS, J., HASSAN, R., SUPROCK, C. A. & ESTERLING, D. 2008. Model - Sensor - Information Technology Integration for Machine Tools. *Proceedings of 2008 NSF Engineering Research and Innovation Conference.* Knoxville, Tennessee.

JERARD, R. B., FUSSELL, B. K., XU, M. & SCHUYLER, C. 2005. Smart Machine Tool Architecture. *Proceedings of 2005 NSF DMII Grantees Conference.* Scottsdale, Arizona.

KACZMAREK, J. 1976. *Principles of Machining by Cutting, Abrasion and Erosion*, Peter Peregrinus Limited.

KAPOOR, S. G., DEVOR, R. E., ZHU, R., GAJJELA, R., PARAKKAL, G. & SMITHEY, D. 1998. Development of mechanistic models for the prediction of machining performance: model building methodology. *Machining Science and Technology,* 2**,** 213-238.

KIM, G. M., CHO, P. J. & CHU, C. N. 2000. Cutting force prediction of sculptured surface ball-end milling using Z-map. *International Journal of Machine Tools & Manufacture,* 40**,** 277–291.

KIM, G. M. & CHU, C. N. 2004. Mean cutting force prediction in ball-end milling using force map method. *Journal of Materials Processing Technology,* 146**,** 303-310.

KIM, G. M., KIM, B. H. & CHU, C. N. 2003. Estimation of cutter deflection and form error in ball-end milling processes. *International Journal of Machine Tools and Manufacture,* 43**,** 917-924.

KLOCKE, F., REUBER, M. & KRATZ, H. 2000. Application of a wavelet-based signal analysis for evaluating the tool state in cutting operations. *Proceeding of 2000 IEEE International Conference on Industrial Electronics, Control and Instrumentation, IECON 2000.* Industrial Electronics Society.

KUO, R. J. & COHEN, P. H. 1999. Multi-sensor integration for on-line tool wear estimation through radial basis function networks and fuzzy neural network. *Neural Networks,* 12**,** 355-370.

LAMIKIZ, A., LO ́PEZ DE LACALLE, L. N., SA ́NCHEZ, J. A. & SALGADO, M. A. 2004. Cutting force estimation in sculptured surface milling. *International Journal of Machine Tools & Manufacture,* 44**,** 1511-1526.

LAZOGLU, I. & LIANG, S. Y. 2000. Modeling of Ball-End Milling Forces With Cutter Axis Inclination. *Journal of Manufacturing Science and Engineering, Transactions of the ASME,* 122**,** 3-11.

LEE, P. & ALTINTAS, Y. 1996. Prediction of ball-end milling forces from orthogonal cutting data. *International Journal of Machine Tools and Manufacture,* 36 1059-1072.

LI, X., LI, H. X., GUAN, X. P. & DU, R. 2004. Fuzzy estimation of feed-cutting force from current measurement - a case study on intelligent tool wear condition monitoring. *IEEE Transactions on Systems, Man, and Cybernetics (Part C),* 34**,** 506-512.

LI, X., LIM, B. S., ZHOU, J. H., HUANG, S., PHUA, S. J. & SHAW, K. C. 2009. Fuzzy Neural Network Modelling for Tool Wear Estimation in Dry Milling Operation. *Annual Conference of the Prognostics and Health Management Society.*

LI, X. Q., WONG, Y. S. & NEE, A. Y. C. 1998. A Comprehensive Identification of Tool Failure and Chatter Using a Parallel Multi-ART2 Neural Network. *Journal of Manufacturing Science and Engineering,* 120**,** 433-442.

NG, E. G., LEE, D. W., DEWES, R. C. & ASPINWALL, D. K. 2000. Experimental Evaluation of Cutter Orientation When Ball Nose End Milling Inconel 718. *Journal of Manufacturing Processes,* 2**,** 108-115.

NIU, Y. M., WONG, Y. S., HONG, G. S. & LIU, T. I. 1998. Multi-Category Classification of Tool Conditions Using Wavelet Packets and ART2 Network. *Journal of Manufacturing Science and Engineering,* 120**,** 807-816.

O'DONNELL, G., YOUNG, P., KELLY, K. & BYRNE, G. 2001. Towards the improvement of tool condition monitoring systems in the manufacturing environment. *Journal of Materials Processing Technology,* 119**,** 133-139.

PAWLAK, Z. 1991. *Rough Sets - Theoretical Aspects of Reasoning about Data*, Kluwer Academic, Dordrecht.

PRICKETT, P. W. & GROSVENOR, R. I. 2007. A microcontroller-based milling process monitoring and management system. *Proc. IMechE Part B: J. Engineering Manufacture,* 221**,** 357-362.

PRICKETT, P. W. & JOHNS, C. 1999. An overview of approaches to end milling tool monitoring. *International Journal of Machine Tools & Manufacture,* 39**,** 105-122.

REHORN, A. G., JIANG, J. & ORBAN, P. E. 2005. State-of-the-art methods and results in tool condition monitoring: a review. *The International Journal of Advanced Manufacturing Technology,* 26**,** 693-710.

RITOU, M., GARNIER, S., FURET, B. & HASCOET, J. Y. 2006. A new versatile in-process monitoring system for milling. *International Journal of Machine Tools & Manufacture,* 46**,** 2026-2035.

SALGADO, D. R. & ALONSO, F. J. 2007. An approach based on current and sound signals for in-process tool wear monitoring. *International Journal of Machine Tools and Manufacture,* 47**,** 2140-2152.

SARHAN, A., SAYED, R., NASSR, A. A. & EL-ZAHRY, R. M. 2001. Interrelationships between cutting force variation and tool wear in end-milling. *Journal of Materials Processing Technology,* 109**,** 229-235.

SATURLEY, P. V. & SPENCE, A. D. 2000. Integration of Milling Process Simulation with On-Line Monitoring and Control. *The International Journal of Advanced Manufacturing Technology,* 16**,** 92-99.

SHEN, L., TAY, F. E. H., QU, L. & SHEN, Y. 2000. Fault diagnosis using Rough Sets Theory. *Computers in Industry,* 43**,** 61-72.

SIDDIQUI, R. A., AMER, W., AHSAN, Q., GROSVENOR, R. I. & PRICKETT, P. W. 2007. Multi-band infinite impulse response filtering using microcontrollers for e-monitoring applications. *Microprocessors and Microsystems,* 31**,** 370-380.

SUBRAHMANYAM, K. V. R. 2009. *Tool Condition Monitoring for Ball Nose Milling - A Model Based Approach.* Degree of Doctor of Philosophy, National University of Singapore.

SUBRAHMANYAM, K. V. R., HUANG, S., WONG, Y. S. & HONG, G. S. 2007. Cutting Force Prediction for Ball Nose Milling. *The International Conference on Product Design and Manufacturing Systems (PDMS'2007).*

SUN, J., HONG, G. S., RAHMAN, M. & WONG, Y. S. 2004a. Identification of feature set for effective tool condition monitoring by acoustic emission sensing. *International Journal of Production Research,* 42**,** 901-918.

SUN, J., HONG, G. S., WONG, Y. S., RAHMAN, M. & WANG, Z. G. 2006. Effective training data selection in tool condition monitoring system. *International Journal of Machine Tools and Manufacture,* 46**,** 218-224.

SUN, J., RAHMAN, M., WONG, Y. S. & HONG, G. S. 2004b. Multiclassification of tool wear with support vector machine by manufacturing loss consideration. *International Journal of Machine Tools and Manufacture,* 44**,** 1179-1187.

SUPROCK, C. A., PIAZZA, J. J. & ROTH, J. T. 2007. Directionally Independent Failure Prediction of End-Milling Tools during Pocketing Maneuvers. *Journal of Manufacturing Science and Engineering, Transactions of the ASME,* 129**,** 770-779.

SWINIARSKI, R. W. & SKOWRON, A. 2003. Rough set methods in feature selection and recognition. *Pattern Recognition Letters,* 24**,** 833-849.

TETI, R., JEMIELNIAK, K., O'DONNELL, G. & DORNFELD, D. 2010. Advanced monitoring of machining operations. *CIRP Annals - Manufacturing Technology,* 59**,** 717-739.

THANGAVEL, K. & PETHALAKSHMI, A. 2009. Dimensionality reduction based on rough set theory: A review. *Applied Soft Computing,* 9**,** 1-12.

VAPNIK, V. N. 1995. *The Nature of Statistical Learning Theory,* New York, Springer-Verlag.

VAPNIK, V. N. 1998. *Statistical Learning Theory,* New York, Wiley.

WANG, L. & GAO, R. X. (eds.) 2006. *Condition Monitoring and Control for Intelligent Manufacturing*: Springer-Verlag London Limited.

WANG, W. H., HONG, G. S., WONG, Y. S. & ZHU, K. P. 2007a. Sensor fusion for online tool condition monitoring in milling. *International Journal of Production Research,* 45**,** 5095-5116.

WANG, X., YANG, J., TENG, X., XIA, W. & JENSEN, R. 2007b. Feature selection based on rough sets and particle swarm optimization. *Pattern Recognition Letters,* 28**,** 459-471.

WIDODO, A. & YANG, B.-S. 2007. Support vector machine in machine condition monitoring and fault diagnosis. *Mechanical Systems and Signal Processing,* 21**,** 2560-2574.

XU, M., JERARD, R. B. & FUSSELL, B. K. 2007. Energy Based Cutting Force Model Calibration for Milling. *Computer-Aided Design & Applications,* 4**,** 341-351.

ZHANG, J. Z. & CHEN, J. C. 2008. Tool condition monitoring in an end-milling operation based on the vibration signal collected through a microcontroller-based data acquisition system. *The International Journal of Advanced Manufacturing Technology,* 39**,** 118-128.

ZHOU, J.-H., PANG, C. K., LEWIS, F. L. & ZHONG, Z.-W. 2009. Intelligent Diagnosis and Prognosis of Tool Wear Using Dominant Feature Identification. *IEEE Transactions on Industrial Informatics,* 5**,** 454-464.

ZHU, K., WONG, Y. S. & HONG, G. S. 2009a. Multi-category micro-milling tool wear monitoring with continuous hidden Markov models. *Mechanical Systems and Signal Processing,* 23**,** 547-560.

ZHU, K., WONG, Y. S. & HONG, G. S. 2009b. Wavelet analysis of sensor signals for tool condition monitoring: A review and some new results. *International Journal of Machine Tools and Manufacture,* 49**,** 537-553.

ZHU, R., DEVOR, R. E. & KAPOOR, S. G. 2003. A Model-based Monitoring and Fault Diagnosis Methodology for Free-Form Surface Machining Process. *Journal of Manufacturing Science and Engineering, Transactions of the ASME,* 125**,** 397-404.

ZHU, R., KAPOOR, S. G. & DEVOR, R. E. 2001. Mechanistic Modeling of the Ball End Milling Process for Multi-Axis Machining of Free-Form Surfaces. *Journal of Manufacturing Science and Engineering, Transactions of the ASME,* 123**,** 369-379.

ZUPERL, U. & CUS, F. 2004. Tool cutting force modeling in ball-end milling using multilevel perceptron. *Journal of Materials Processing Technology,* 153-154**,** 268-275.